FEATURE ARTICLE

The Semiclassical Initial Value Representation: A Potentially Practical Way for Adding Quantum Effects to Classical Molecular Dynamics Simulations

William H. Miller

Department of Chemistry and Kenneth S. Pitzer Center for Theoretical Chemistry, University of California, and Chemical Sciences Division, Lawrence Berkeley National Laboratory, Berkeley, California 94720-1460

The semiclassical (SC) initial value representation (IVR) provides a potentially practical way for adding quantum mechanical effects to classical molecular dynamics (MD) simulations of the dynamics of complex molecular systems (i.e., those with many degrees of freedom). It does this by replacing the nonlinear boundary value problem of semiclassical theory by an average over the initial conditions of classical trajectories. This paper reviews the background and rebirth of interest in such approaches and surveys a variety of their recent applications. Special focus is on the ability to treat the dynamics of complex systems, and in this regard, the forward−backward (FB) version of the approach is especially promising. Several examples of the FB-IVR applied to model problems of many degrees of freedom show it to be capable of describing quantum effects quite well and also how these effects are quenched when some of the degrees of freedom are averaged over ("decoherence").

I. Introduction

It is well-known that classical molecular dynamics (MD) simulations are widely used nowadays to describe a variety of dynamical processes in complex molecular systems, e.g., chemical reactions in solution, in (or on) solids, in clusters, and in biomolecular environments. Nature, however, obeys quantum rather than classical mechanics, so that it would clearly be desirable to have theoretical approaches capable of including quantum coherence and tunneling effects into classical MD, even approximately, to show when they are important and when they are not. For some processes, particularly those involving hydrogen atom motion, one can reasonably expect quantum effects to be significant. Solvation dynamics, for example, primarily involves the reorientation of the dipoles of water molecules, and this is almost exclusively hydrogen atom motion (i.e., the rotation of water molecules). Also, as soon as one allows the OH (or CH or NH) bond to become dynamically active (most classical MD simulations use rigid-rotor H_2O molecules), as one obviously must when these bonds are broken and participate as a reactant or product in a chemical reaction, quantum effects may become significant (recall that $\hbar\omega$ for an OH stretch vibration is ∼18 times kT at room temperature). Furthermore, any process that involves transitions between different Born−Oppenheimer electronic states—almost always the case in photochemistry—necessarily involves quantum mechanics for the nonadiabatic dynamics of the electronic degrees of freedom, and one must somehow combine this with a consistent description of the dynamics of nuclear motion.

Since a complete quantum treatment of the dynamics[1] of many degrees of freedom is not feasible, there are several ways one can proceed in order to model these phenomena theoretically. One is to employ various mixed quantum−classical models,[2] whereby a few of the most important degrees of freedom are treated quantum mechanically and the remaining (many) degrees of freedom treated by classical mechanics. There are many variations on this idea, and they have been useful in a variety of applications. As with any approximate model, however, there are shortcomings of such approaches, related primarily to the ultimate inconsistency of describing different degrees of freedom differently. For thermal ensembles, there are also several ways of defining an effective potential[3] that includes some quantum effects and on which classical trajectories are then evolved.

Another strategy, which has had a rebirth of interest recently and is the subject of this paper, is to treat all degrees of freedom (even the electronic degrees of freedom involved in a nonadiabatic process) semiclassically (SC). Much work[4,5] in the early 1970s showed how numerically computed classical trajectories for multidimensional systems could be used semiclassically and that such a theory provides an approximate description of *all* quantum effects in molecular dynamics—interference (coherence), tunneling, selection rules due to identical particle symmetry, and quantization of bounded motion—since they all arise ultimately from the superposition of probability amplitudes, which is contained in this semiclassical description. Many applications were carried out at that time, primarily to gas-phase molecular collision problems, illustrating these ideas and showing that the semiclassical description is often very good even when quantum effects are quite large. Since, as noted above, classical MD is now quite feasible even for complex molecular systems, and since SC theory only requires classical trajectories as input, it should therefore be possible in principle to use SC theory to add quantum effects to classical MD simulations of complex systems.

The first step toward changing "in principle" into "in practice" is use of the initial value representation (IVR). Though the basic

Feature Article

J. Phys. Chem. A, Vol. 105, No. 13, 2001 **2943**

IVR idea—i.e., of converting the SC nonlinear boundary value, or "root search" problem, into an integral over initial conditions—was introduced many years ago,[4b] it is recent work[6−15] by several groups that has resurrected interest in it as a simulation tool. The purpose of this paper is to review the basic IVR approach and some of its recent applications, with special emphasis on its potential for being able to describe quantum effects in complex molecular systems, i.e., those with many degrees of freedom. The ultimate goal of this work is to be able to implement classical trajectory simulations in a way that can incorporate quantum effects in a completely non-ad hoc fashion.

Section II first reviews the basic IVR idea and its connection with older SC theory, and section III shows how the description can be generalized to include the electronic degrees of freedom in nonadiabatic processes on an equal footing with those of the nuclei. Section IV then surveys recent applications of the SC-IVR to simple systems (i.e., those with a few degrees of freedom). For simple systems, one can compare SC-IVR results with accurate quantum calculations, and these comparisons provide strong evidence that the SC-IVR approach, to the extent that it can be applied, provides an excellent description of quantum effects in essentially all cases.

The main challenge, therefore, is one of implementation; i.e., can one in fact carry out SC-IVR calculations for molecular systems with many degrees of freedom? Section V therefore focuses explicitly on the evaluation of time correlation functions,[16] which are the quantities of dynamical interest for complex systems. Of particular interest in this regard is the forward−backward (FB) version of the IVR, which emerges as the simplest version of the theory that is capable of describing true quantum coherence/interference effects in molecular dynamics. Several recent applications of the FB-IVR approach are discussed there, showing unequivocally that it is able to describe quantum interference effects (from which all quantum effects ultimately arise) in systems with many degrees of freedom and also how these effects are (partially) quenched when the coupling to "environmental" degrees of freedom is sufficiently large.

II. Basic Initial Value Representation Idea

The basic IVR idea[4b,5c,d,17] can be illustrated by considering a generic matrix element of the time evolution operator (propagator)

$$K_{\mathbf{n}_2,\mathbf{n}_1}(t) \equiv \langle \psi_{\mathbf{n}_2} | e^{-i\hat{H}t/\hbar} | \psi_{\mathbf{n}_1} \rangle =$$
$$\int d\mathbf{x}_1 \int d\mathbf{x}_2 \, \psi_{\mathbf{n}_2}(\mathbf{x}_2)^* \psi_{\mathbf{n}_1}(\mathbf{x}_1) \langle \mathbf{x}_2 | e^{-i\hat{H}t/\hbar} | \mathbf{x}_1 \rangle \quad (2.1)$$

which is the probability amplitude for a transition from state $\mathbf{n}_1$ at time zero to state $\mathbf{n}_2$ at time t. Use of the standard semiclassical (Van Vleck[18]) approximation for the coordinate representation of propagator gives

$$K_{\mathbf{n}_2,\mathbf{n}_1}(t) = \sum_{\text{roots}} \int d\mathbf{x}_1 \int$$
$$d\mathbf{x}_2 \, \psi_{\mathbf{n}_2}(\mathbf{x}_2)^* \psi_{\mathbf{n}_1}(\mathbf{x}_1) \left[(2\pi i\hbar)^F \left| \frac{\partial \mathbf{x}_2}{\partial \mathbf{p}_1} \right| \right]^{-1/2} e^{iS_t(\mathbf{x}_2,\mathbf{x}_1)/\hbar} \quad (2.2)$$

where $S_t(\mathbf{x}_2,\mathbf{x}_1)$ is the classical action along the trajectory that goes from $\mathbf{x}_1$ to $\mathbf{x}_2$ in time t

$$S_t(\mathbf{x}_2,\mathbf{x}_1) = \int_0^t dt' \, \mathbf{p}(t')\dot{\mathbf{x}}(t') - H(\mathbf{p}(t'),\mathbf{x}(t')) \quad (2.3)$$
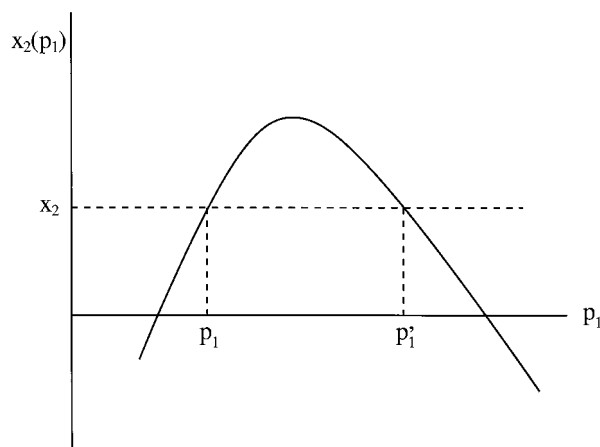

Figure 1. Sketch of the final position x_2 of a classical trajectory as a function of its initial momentum p_1 (for a fixed value of the initial position x_1), indicating that there may be more than one classical trajectory (here two) that are determined by the boundary conditions (x_2,x_1).

where $H(\mathbf{p},\mathbf{x})$ is the classical Hamiltonian of the system. To apply eq 2.2 as written, one needs to solve a nonlinear boundary value problem (the root search problem): if $\mathbf{x}_2(\mathbf{p}_1,\mathbf{x}_1)$ is the coordinate at time t that evolves from the initial condition $(\mathbf{p}_1,\mathbf{x}_1)$ at $t = 0$, then for a given $\mathbf{x}_1$, one must find the values of $\mathbf{p}_1$ that satisfy

$$x_2(\mathbf{p}_1,\mathbf{x}_1) = \mathbf{x}_2 \quad (2.4)$$

In general, there will be multiple roots, as indicated graphically in Figure 1, and the summation in eq 2.2 is over all such roots. The Jacobian factor in eq 2.2 is evaluated at the root of eq 2.4, and one must take the appropriate branch of the square root in eq 2.2 (i.e., the Maslov index).

In the older semiclassical work[4,5] of the early 1970s, one usually proceeded further by introducing semiclassical approximations for the wave functions $\psi_n(\mathbf{x})$ in eq 2.2 (i.e., by using action−angle variables) and also evaluating the integrals over $\mathbf{x}_1$ and $\mathbf{x}_2$ via the stationary phase approximation (SPA). These approximations, which formally introduce no additional error to that already contained in the semiclassical approximation to the coordinate matrix of the propagator, give the following "primitive" semiclassical result for the matrix element

$$K_{\mathbf{n}_2,\mathbf{n}_1}(t) = \sum_{\text{roots}} \left[(-2\pi i\hbar)^F \left| \frac{\partial \mathbf{n}_2}{\partial \mathbf{q}_1} \right| \right]^{-1/2} e^{iS_t(\mathbf{n}_2,\mathbf{n}_1)/\hbar} \quad (2.5a)$$

where $(\mathbf{n},\mathbf{q})$ are the action−angle variables (that have replaced the Cartesian variables $(\mathbf{p},\mathbf{x})$) and the action $S_t(\mathbf{n}_2,\mathbf{n}_1)$ is

$$S_t(\mathbf{n}_2,\mathbf{n}_1) = \int_0^t dt' \, [-\mathbf{q}(t')\dot{\mathbf{n}}(t') - H(\mathbf{n}(t'),\mathbf{q}(t'))] \quad (2.5b)$$

Here the initial and final action variables, $\mathbf{n}_1$ and $\mathbf{n}_2$—the classical counterpart to the quantum numbers of the initial and final states—are the boundary values that determine the appropriate classical trajectories, i.e., those that satisfy

$$\mathbf{n}_2(\mathbf{q}_1,\mathbf{n}_1) = \mathbf{n}_2 \quad (2.5c)$$

The strategy of the IVR approach, however, is *not* to perform the $\mathbf{x}_1$ and $\mathbf{x}_2$ integrals in eq 2.2 via the SPA but rather to carry them out numerically; i.e., one makes the semiclassical approximation to the propagator in the (Cartesian) coordinate (or

momentum) representation and then carries out any further manipulations with it fully quantum mechanically.[19] An important simplification of eq 2.2—the basic IVR "trick"—is then possible: inside the integral over $\mathbf{x}_1$, the integration over $\mathbf{x}_2$ is changed to that over $\mathbf{p}_1$

$$\sum_{\text{roots}} \int d\mathbf{x}_2 = \int d\mathbf{p}_1 \left| \frac{\partial \mathbf{x}_2(\mathbf{x}_1, \mathbf{p}_1)}{\partial \mathbf{p}_1} \right| \qquad (2.6)$$

where the Jacobian comes from this change of integration variables. As is clear from Figure 1, integration over $\mathbf{p}_1$ corresponds to integration over $\mathbf{x}_2$ and summation over all multiples roots. Equation 2.2 thus becomes

$$K_{\mathbf{n}_2, \mathbf{n}_1}(t) = \int d\mathbf{x}_1 \int d\mathbf{p}_1 \left[\left| \frac{\partial \mathbf{x}_t(\mathbf{x}_1, \mathbf{p}_1)}{\partial \mathbf{p}_1} \right| \middle/ \right.$$
$$\left. (2\pi i\hbar)^F \right]^{1/2} e^{iS_t(\mathbf{x}_1, \mathbf{p}_1)/\hbar} \psi_{\mathbf{n}_2}(\mathbf{x}_t)^* \psi_{\mathbf{n}_1}(\mathbf{x}_1), \quad (2.7)$$

where $S_t(\mathbf{x}_1, \mathbf{p}_1) \equiv S_t(\mathbf{x}_t(\mathbf{x}_1, \mathbf{p}_1), \mathbf{x}_1)$ and $\mathbf{x}_t(\mathbf{x}_1, \mathbf{p}_1)$ is now written for $\mathbf{x}_2(\mathbf{x}_1, \mathbf{p}_1)$.

Equation 2.7 is the simplest example of an IVR. The nonlinear boundary value problem has been replaced by an integral over the phase space of initial conditions, something that is more amenable for application to systems of many degrees of freedom (if Monte Carlo methods can be utilized for preforming the phase space integration). It is also useful that the Jacobian factor $(\partial \mathbf{x}_t/\partial \mathbf{p}_1)$ now appears in the numerator in eq 2.7, rather than the denominator as in eq 2.2, since it can go through zero for various values of the integration variables. Equation 2.7 still has all the interference structure that is the hallmark of semiclassical theory; e.g., if the integrals in eq 2.7 were all evaluated by the stationary phase approximation and WKB wave functions were used for ψ_1 and ψ_2, the primitive semiclassical result (eq 2.5) would be obtained, with interference between different stationary phase trajectories, etc. The IVR also provides an approximate description of classically forbidden processes ("dynamical tunneling"[20a]), where there are no real stationary phase contributions to the integral. In fact, this was the first application[4b] of an IVR and the principle reason it was originally introduced, i.e., as a way to treat classically forbidden processes with real-valued trajectories.

Equation 2.7 can also be written in Dirac notation

$$\langle \psi_{\mathbf{n}_2} | e^{-i\hat{H}t/\hbar} | \psi_{\mathbf{n}_1} \rangle = \int d\mathbf{x}_0 \int d\mathbf{p}_0 \left[\left| \frac{\partial \mathbf{x}_t(\mathbf{x}_0, \mathbf{p}_0)}{\partial \mathbf{p}_0} \right| \middle/ \right.$$
$$\left. (2\pi i\hbar)^F \right]^{1/2} e^{iS_t(\mathbf{x}_0, \mathbf{p}_0)/\hbar} \langle \psi_{\mathbf{n}_2} | \mathbf{x}_t \rangle \langle \mathbf{x}_0 | \psi_{\mathbf{n}_1} \rangle \quad (2.8)$$

where now $(\mathbf{x}_0, \mathbf{p}_0)$ denotes the initial conditions for the trajectory, $\mathbf{x}_t = \mathbf{x}_t(\mathbf{x}_0, \mathbf{p}_0)$ is the time-evolved position, etc., and one can delete the initial and final states from eq 2.8 to have an explicit representation of the propagator itself in terms of Dirac position eigenstates

$$e^{-i\hat{H}t/\hbar} =$$
$$\int d\mathbf{x}_0 \int d\mathbf{p}_0 \left[\left| \frac{\partial \mathbf{x}_t(\mathbf{x}_0, \mathbf{p}_0)}{\partial \mathbf{p}_0} \right| / (2\pi i\hbar)^F \right]^{1/2} e^{iS_t(\mathbf{x}_0, \mathbf{p}_0)/\hbar} |\mathbf{x}_t\rangle\langle\mathbf{x}_0| \quad (2.9)$$

Equation 2.9 is the Cartesian coordinate IVR; if one proceeded similarly but with momentum space wave functions, then the (Cartesian) momentum version would be obtained

$$e^{-i\hat{H}t/\hbar} =$$
$$\int d\mathbf{x}_0 \int d\mathbf{p}_0 \left[\left| \frac{\partial \mathbf{p}_t(\mathbf{x}_0, \mathbf{p}_0)}{\partial \mathbf{x}_0} \right| / (-2\pi i\hbar)^F \right]^{1/2} e^{i\tilde{S}_t(\mathbf{x}_0, \mathbf{p}_0)/\hbar} |\mathbf{p}_t\rangle\langle\mathbf{p}_0|$$
$$(2.10a)$$

where $\mathbf{p}_t(\mathbf{x}_0, \mathbf{p}_0)$ is the time-evolved momentum and the action integral in momentum space is given by[4d]

$$\tilde{S}_t(\mathbf{x}_0, \mathbf{p}_0) = \int_0^t dt' \, [-\mathbf{x}(t')\dot{\mathbf{p}}(t') - H(\mathbf{p}(t'), \mathbf{x}(t'))] \quad (2.10b)$$

A particularly useful contribution was made by Herman and Kluk[6a] (HK) in showing that a similar expression pertains also for coherent states $|\mathbf{p}_0, \mathbf{x}_0\rangle$, which are hybrid states, intermediate between position and momentum eigenstates

$$e^{-i\hat{H}t/\hbar} =$$
$$(2\pi\hbar)^{-F} \int d\mathbf{x}_0 \int d\mathbf{p}_0 \, C_t(\mathbf{x}_0, \mathbf{p}_0) \, e^{iS_t(\mathbf{x}_0, \mathbf{p}_0)/\hbar} |\mathbf{p}_t, \mathbf{x}_t\rangle\langle\mathbf{p}_0, \mathbf{x}_0|$$
$$(2.11a)$$

Here S_t is the same action integral as that in eq 2.3, and the HK prefactor is

$$C_t(\mathbf{x}_0, \mathbf{p}_0) = \left| \frac{1}{2} \left(\frac{\partial \mathbf{x}_t}{\partial \mathbf{x}_0} + \frac{\partial \mathbf{p}_t}{\partial \mathbf{p}_0} + \frac{\hbar\gamma}{i} \frac{\partial \mathbf{x}_t}{\partial \mathbf{p}_0} + \frac{i}{\hbar\gamma} \frac{\partial \mathbf{p}_t}{\partial \mathbf{x}_0} \right) \right|^{1/2} \quad (2.11b)$$

The coordinate space wave functions of the (Glauber) coherent states[21] are given by

$$\langle \mathbf{x} | \mathbf{p}_0, \mathbf{x}_0 \rangle = \left(\frac{\gamma}{\pi} \right)^{F/4} e^{-(\gamma/2)|\mathbf{x} - \mathbf{x}_0|^2} e^{i\mathbf{p}_0(\mathbf{x} - \mathbf{x}_0)/\hbar} \quad (2.12)$$

and similarly for $\langle \mathbf{x} | \mathbf{p}_t, \mathbf{x}_t \rangle$; they become position eigenstates as $\gamma \to \infty$ and momentum eigenstates as $\gamma \to 0$, in which limit eq 2.11 reduces to eqs 2.9 and 2.10, respectively. Their usefulness is that they are localized in both coordinate and momentum space. Coherent states are the "frozen Gaussian" version of the semiclassical wave packet methodology developed by Heller[20b,c] and fruitfully applied by him to many problems over the years. It was this frozen Gaussian (i.e., fixed γ) model that motivated Herman and Kluk in obtaining eq 2.11. Kay[8a] has also described the generalization of eq 2.11, where the coherent state parameter γ is a matrix and different for the initial and final coherent states.

III. Inclusion of Electronic Degrees of Freedom

It is not advocated (at least here) that one describes the physical coordinates and momenta of electrons semiclassically, but the collective degrees of freedom associated with a finite manifold of electronic states can be included in the SC-IVR approach by using the "classical electron analog" model of Meyer and Miller (MM).[22] If $\mathbf{X}$ and $\mathbf{P}$ denote the (Cartesian) coordinates and momenta of the nuclei and (n_k, q_k), $k = 1, ..., N$ the classical action–angle variables corresponding to a set of N electron states, then MM's classical Hamiltonian for the complete nuclear-electronic system is

$$H(\mathbf{P}, \mathbf{X}, \mathbf{n}, \mathbf{q}) = \frac{\mathbf{P}^2}{2\mu} + \sum_{k=1}^N n_k H_{kk}(\mathbf{X}) +$$
$$\sum_{\substack{k,k'=1 \\ k' \neq k}}^N H_{kk'}(\mathbf{X}) \left[\left(n_k + \frac{1}{2} \right)\left(n_{k'} + \frac{1}{2} \right) \right]^{1/2} \cos(q_k - q_{k'}) \quad (3.1)$$

where $\{H_{k,k'}(\mathbf{X})\}$ is the diabatic[23] electronic Hamiltonian matrix

(assumed here to be real) which characterizes the N electronic states; it is assumed to come from an "honest" quantum mechanical electronic structure calculation for fixed nuclear coordinates $\mathbf{X}$. MM used this Hamiltonian, eq 3.1, within the "quasiclassical" model:[24] i.e., the initial conditions were set to quantized initial values ($n_i(t_1) = 1$ if state i is the initial electronic state, $n_k(t_1) = 0$ for $k \neq i$, with all angle variables $q_k(t_1)$ chosen randomly from the interval $(0,2\pi)$, and similarly for the bound nuclear degrees of freedom), and the final action variables were histogrammed to determine the distribution of final electronic (and nuclear) states. The primary motivation for this was to have an approach which treated electronic and nuclear dynamics on an equal footing. A variety of applications in the early 1980s gave reasonably good results for a variety of electronically nonadiabatic processes (F* + H$_2$ ($j = 0$) → F + H$_2$ ($j = 2$),[25] Br* + H$_2$ ($v = 0$) → Br + H$_2$ ($v = 1$),[26] Na + I → Na$^+$ + I$^-$,[27] ...). It is appreciated, though, that histogramming an action variable into quantum number "bins", when it only spans a range from $-1/2$ to $3/2$, is very crude at best, and the model thus does not always give accurate results.[28]

One now proposes to upgrade the description to the semiclassical level,[29] and from the discussion in section II, it is clear that one first transforms from the electronic action–angle variables in eq 3.1 to the corresponding Cartesian-like electronic coordinates and momenta

$$x_k = \sqrt{n_k + \tfrac{1}{2}}\, \cos q_k \qquad (3.2a)$$

$$p_k = -\sqrt{n_k + \tfrac{1}{2}}\, \sin q_k \qquad (3.2b)$$

The classical Hamiltonian[30] thus becomes

$$H(\mathbf{P},\mathbf{X},\mathbf{p},\mathbf{x}) = \frac{\mathbf{P}^2}{2\mu} + \sum_{k=1}^{N}\frac{1}{2}(p_k^2 + x_k^2 - 1)H_{kk}(\mathbf{X}) + \sum_{k<k'=1}^{N}(p_kp_{k'} + x_kx_{k'})H_{kk'}(\mathbf{X}) \quad (3.3)$$

where it is seen that the electronic degrees of freedom appear as harmonic oscillators, one for each electronic state. The coordinate space wave functions for these N electronic states are thus given by

$$\Phi_k(\mathbf{x}) = \phi_1(x_k) \prod_{\substack{k'=1 \\ k' \neq k}}^{N} \phi_0(x_{k'}) \qquad (3.4)$$

where $\phi_0(x)$ and $\phi_1(x)$ are the ordinary one-dimensional harmonic oscillator wave functions for the ground and first excited state. Since the sum of the N quanta, $\sum_{k=1}^{N} n_k$, is a conserved quantity (both classical and quantum mechanically) for the Hamiltonian of eq 3.3, this is a complete set of states in the manifold $\sum_{k=1}^{N} n_k = 1$; i.e., the N "electronic" states correspond to one quantum of excitation (essentially the probability) being in one of the N electronic modes.

It is interesting to note that if the Hamiltonian of eq 3.3 were upgraded to a full quantum description, then it provides an exact representation of the full nuclear-N electronic state system. This is most directly apparent from the deviation given by Stock and Thoss[31] and can also be readily verified by constructing the matrix of the electronic oscillator Hamiltonian for fixed nuclei

$$H_{el}(\hat{\mathbf{p}},\hat{\mathbf{x}};\mathbf{X}) = \sum_{k=1}^{N}\frac{1}{2}(\hat{p}_k^2 + \hat{x}_k^2 - 1)H_{kk}(\mathbf{X}) + \sum_{k<k'=1}^{N}(\hat{p}_k\hat{p}_{k'} + \hat{x}_k\hat{x}_{k'})H_{kk'}(\mathbf{X}) \quad (3.5a)$$

in the basis of the N states of eq 3.4; an elementary calculation shows that

$$\langle \Phi_k | H_{el} | \Phi_{k'} \rangle = H_{kk'}(\mathbf{X}) \qquad (3.5b)$$

and since the matrix of the electronic oscillator Hamiltonian is identical to the original diabatic electronic matrix, the resulting quantum mechanics must be the same. At the full quantum level of description, therefore, eq 3.3 is not an approximation to the electronic–nuclear system, but rather a particular representation of it.[31] The approximation is that we now proceed to treat it semiclassically.

It is a straightforward matter to apply the SC-IVR approach of section II to the classical Hamiltonian of eq 3.3. If $\chi_1(\mathbf{R})$ and $\chi_2(\mathbf{R})$ denote the initial and final nuclear wave functions, then the SC-IVR expression for a typical vibronic (i.e., electronic-nuclear) transition amplitude is the generalization of eq 2.7

$$S_{2,1}(t) = \int d\mathbf{x}_1\, d\mathbf{X}_1 \int d\mathbf{p}_1\, d\mathbf{P}_1 \left[\frac{\partial(\mathbf{x}_t,\mathbf{X}_t)}{\partial(\mathbf{p}_1,\mathbf{P}_1)}/(2\pi i\hbar)^{F+N}\right]^{1/2} \chi_2^*(\mathbf{X}_t)\Phi_{k_2}^*(\mathbf{x}_t)\Phi_{k_1}(\mathbf{x}_1)\chi_1(\mathbf{X}_1)\, e^{iS_t(\mathbf{x}_1,\mathbf{p}_1,\mathbf{X}_1,\mathbf{P}_1)/\hbar} \quad (3.6)$$

where $\mathbf{x}_t(\mathbf{x}_1,\mathbf{p}_1,\mathbf{X}_1,\mathbf{P}_1)$ and $\mathbf{X}_t(\mathbf{x}_1,\mathbf{p}_1,\mathbf{X}_1,\mathbf{P}_1)$ are the coordinates at time t that evolve along the classical trajectory with the indicated initial conditions and S_t the corresponding action integral. The classical trajectories here are for the full set of N electronic and F nuclear degrees of freedom (in the MM spirit) obtained from the classical Hamiltonian of eq 3.3. As noted before, this approach has the desirable feature of treating the electronic and nuclear degrees of freedom on an equal basis, thus avoiding any inconsistencies that arise in trying to mix a quantum description of some degrees of freedom with a classical description of others.

It is also interesting to note that the above SC-IVR approach includes the Pechukas model[32] for treating electronically nonadiabatic processes. In this approach, one begins with the (formally exact) Feynman path integral expression for the electronic–nuclear time evolution operator

$$\langle \mathbf{x}_2\mathbf{X}_2 | e^{-iHt/\hbar} | \mathbf{x}_1\mathbf{X}_1 \rangle = \int_{\mathbf{X}_1}^{\mathbf{X}_2} D\mathbf{X}(t) \int_{\mathbf{x}_1}^{\mathbf{x}_2} D\mathbf{x}(t)\, e^{iS[\mathbf{x}(t),\mathbf{X}(t)]/\hbar} \quad (3.7)$$

and imagines first evaluating (exactly) the path integral over the electronic degrees of freedom, whereby the vibronic amplitude becomes

$$S_{2,1}(t) = \int d\mathbf{X}_2 \int d\mathbf{X}_1\, \chi_2(\mathbf{X}_2)^*\chi_1(\mathbf{X}_1) \int_{\mathbf{X}_1}^{\mathbf{X}_2} D\mathbf{X}(t) \exp\left[\frac{i}{\hbar}\int_0^t dt'\,\frac{1}{2}\mu\dot{\mathbf{X}}(t')^2\right] K_{2,1}[\mathbf{X}(t)] \quad (3.8)$$

where $K_{2,1}[\mathbf{X}(t)]$ is the electronic transition amplitude as a functional of the nuclear path $\mathbf{X}(t)$. Up to this point, the formulation is exact, but Pechukas now evaluates the nuclear path integral semiclassically, i.e., via the functional version of the stationary-phase approximation. This determines an effective nuclear trajectory. The SC-IVR approach, however—if it were

implemented in this two stage fashion—would generate the electronic transition amplitude $K_{2,1}[\mathbf{X}(t)]$ exactly; this is because for a fixed nuclear trajectory the electronic Hamiltonian of eq 3.5a is a time-dependent quadratic Hamiltonian, for which the semiclassical approximation is exact. The SC-IVR model then does a better job of treating the nuclear degrees of freedom by using the IVR rather than the stationary phase approximation. In practice, of course, one does not implement the SC-IVR model in this two-stage manner, but rather treats the nuclear and electronic dynamics simultaneously. One (desirable) consequence of this is that there are no nonlocal (in time) forces[32] to deal with.

IV. Applications to Simple Systems

There have been a number of applications of the SC-IVR approach by a number of different research groups to a variety of simple systems (i.e., those with a small number of degrees of freedom) that illustrate its usefulness and the typical accuracy one can expect. Here we discuss a selected set of these, which have used either the coordinate-space (i.e., Van Vleck) IVR or the coherent-state (Herman—Kluk) version.

Eigenvalue spectra and photodissociation cross sections involve a diagonal matrix element of the microcanonical density operator

$$I(E) \equiv \langle \chi | \delta(E - \hat{H}) | \chi \rangle \qquad (4.1a)$$

which can be expressed as the Fourier transform of the matrix element of the propagator

$$I(E) = \frac{1}{\pi\hbar} Re \int_0^\infty dt \, e^{iEt/\hbar} \langle \chi | e^{-i\hat{H}t/\hbar} | \chi \rangle \qquad (4.1b)$$

The matrix element $\langle \chi | e^{-i\hat{H}t/\hbar} | \chi \rangle$ is thus evaluated by the SC-IVR procedure, eq 2.7 or 2.11, and then integrated over time as in eq 4.1b to obtain $I(E)$. For a bounded molecular system, the formal expression for $I(E)$ is

$$I(E) = \sum_n |\langle \chi | \psi_n \rangle|^2 \delta(E - E_n) \qquad (4.2)$$

where $\{E_n\}$ and $\{|\psi_n\rangle|\}$ are the eigenvalues and eigenfunctions of $\hat{H}$, so that peaks in $I(E)$ identify eigenvalues. (Typically, a convergence factor, e.g., $\exp[-(1/2)\Delta E^2 t^2/\hbar^2]$, is included in the time integral to accelerate its convergence, and the delta function peaks of eq 4.2 become Gaussians, $\exp[-(1/2)(E - E_n)^2/\Delta E^2]$.)

Tomsovic and Heller[9c] have calculated such eigenvalue spectra for the two-dimensional stadium billiard (using the Van Vleck IVR) and found excellent results, even up to very highly excited states for which the level density becomes large. (This required the use of some very clever techniques for carrying out the phase space integral that are special for billiard (i.e., hard wall) systems.) This example shows that the semiclassical matrix element of the propagator can be accurate for long time, much longer then had previously been expected, and even when the classical dynamics is highly chaotic.

The eigenvalue spectrum of the HCl dimer (treating each monomer as a rigid rotor) has been calculated by Sun and Miller,[10i] specifically, the lowest few vibrational eigenvalues of each molecular symmetric (A^+, A^-, B^+, and B^-). Agreement with quantum mechanical calculations (with the same potential energy function) was quite good (to $1-2$ cm^{-1}), even for the tunneling splitting associated with the symmetrical hydrogen bond flipping, i.e., Cl$-$H$\cdots$Cl$-$H $\rightarrow$ H$-$Cl$\cdots$H$-$Cl ($\Delta E_{QM} =$ 16 cm^{-1}, $\Delta E_{SC} = 18$ cm^{-1}).

Photodetachment spectra (i.e., photoelectron spectra of negative ions) have been calculated by Brewer, Hulme, and Manolopoulos[11c] for I$^-$(Ar)$_n$, $n = 2-6$; this is essentially the $I(E)$ of eq 4.1, where $|\chi\rangle$ is the initial (ground) vibrational state of the negative ion and $\hat{H}$ the Hamiltonian for the (dissociative) neutral molecular system. Very good results were obtained, and it was impressive that such a relatively large system (up to 15 degrees of freedom) could be treated (though many of these were very weakly coupled harmonic modes).

An example involving electronically nonadiabatic dynamics, i.e., the electronic—nuclear Hamiltonian of section III, was the photodissociation of ozone treated by Batista and Miller.[10g] Here $|\chi\rangle$ is the ground vibrational state of ozone (in its ground electronic state), and the Hamiltonian $\hat{H}$ consists of two excited electronis states, coupled through a conical intersection, along with the nuclear degrees of freedom. Agreement of the SC-IVR results with quantum calculations[33] for the same system were very good. Similar calculations by Coronado et al.[10v] for the photodissociation of ICN, involving nonadiabatic dynamics of two coupled excited electronic states, also gave excellent agreement with quantum calculations; a very impressive calculation of this type for photoexcitation of pyrazine to the excited S_2 state, which is coupled to the S_1 state via a conical intersection, was carried out by Thoss et al.[10w] including all 24 vibrational degrees of freedom, resulting in very good agreement with quantum multiconfiguration time-dependent Hartree (MCT-DH) calculations.

State-to-state scattering calculations are also possible by using the formal quantum mechanical expression for the S-matrix in terms of the propagator[4d]

$$S_{\mathbf{n}_2, \mathbf{n}_1}(E) = -\sqrt{v_1 v_2} \, e^{-i(k_1 R_1 + k_2 R_2)} \int_0^\infty$$
$$dt \, e^{iEt/\hbar} \langle R_2 \phi_{\mathbf{n}_2} | e^{-i\hat{H}t/\hbar} | R_1 \phi_{\mathbf{n}_1} \rangle \quad (4.3)$$

where $\{\phi_n(r)\}$ is the asymptotic internal eigenfunctions of the collision partners and R the (Jacobi) coordinate for relative translational motion; E is the total energy, $k_i = \sqrt{2\mu(E - \epsilon_{n_i})/\hbar^2}$ the translational wavevectors, and $v_i = \hbar k_i/\mu$ the translational velocities. This can be put into standard IVR form by adding the factor $\delta(R_2 - R_f)$ to the integrand and integrating over R_2, making the IVR transformation alá eq 2.6, and then doing the t-integral by virtue of the factor $\delta(R_t - R_f)$, giving finally

$$S_{\mathbf{n}_2, \mathbf{n}_1}^{IVR}(E) = -e^{-i(k_1 R_1 + k_2 R_2)} \int d\mathbf{r}_0 \int d\mathbf{p}_0 \int dP_0 \left[\left| \frac{\partial(R_t, \mathbf{r}_t)}{\partial(P_0, \mathbf{p}_0)} \right| / \right.$$
$$\left. (2\pi i\hbar)^F \right]^{1/2} e^{i(Et + S_t)/\hbar} \phi_{\mathbf{n}_2}(\mathbf{r}_t)^* \phi_{\mathbf{n}_1}(\mathbf{r}_0) \mu \sqrt{v_1 v_2}/P_t \quad (4.4)$$

where $R_0 = R_1$ and t is determined by the time that $R_t = R_2$. Skinner and Miller[10o] carried out such calculations for the standard model of inelastic scattering, the collinear He + H$_2$ system first studied by Secrest and Johnson[34] many years ago. Agreement with the correct quantum results is essentially quantitative, following the interference structure in the transition probabilities $P_{n_2, n_1} \equiv |S_{n_2, n_1}|^2$ as a function of final vibrational quantum number.

Garashchuk, Grossmann, and Tannor[12] have carried out similar scattering calculations (but using the HK coherent state IVR) for the collinear H + H$_2$ $\rightarrow$ H$_2$ + H reaction, here the primary interest being to see how well the SC-IVR approach can describe the resonance structure in the energy dependence of the reaction probability. It has long been realized that,[35,36] from a semiclassical point of view, resonance structure is an

Feature Article

J. Phys. Chem. A, Vol. 105, No. 13, 2001 **2947**

interference effect between different trajectories that are temporarily trapped in the collision complex (just as discrete eigenvalues themselves are the result of interference between different trajectories that are trapped forever in a bounded molecular system). As such, they should be describable within the SC-IVR approach, and it is indeed encouraging to see that the resonance structure from Garashchuk et al.'s semiclassical calculations is in very good agreement with the correct quantum structure. It is another important illustration of the fact that the SC-IVR model is capable of providing a usefully accurate description of quantum effects in chemical dynamics.

Application of the SC-IVRs of section II, eq 2.9 or 2.11, to compute spectral densities $I(E)$ (eq 4.1), S-matrixes (eq 4.3), or any other quantum expression involving the propagator, is thus very straightforward in principle. The "only" computational difficulty is that it involves evaluating a multidimensional integral (over the phase space of initial conditions) of an oscillatory integrand. To accomplish this, the applications above have all used variations of "filtering" or stationary phase Monte Carlo methods[37] to dampen the oscillations of the integrand. Consider, for example, a generic integral of the form

$$I = \int d\mathbf{x}\, A(\mathbf{x})\, e^{iS(\mathbf{x})} \tag{4.5}$$

The modified Filinov approach[37b] replaces this by

$$I(c) = \int d\mathbf{x}\, A(\mathbf{x})\, e^{iS(\mathbf{x})}\, e^{-(c/2)|(\partial S/\partial \mathbf{x})|^2} |\mathbf{I} + ic\frac{\partial^2 S}{\partial \mathbf{x}\,\partial \mathbf{x}}|^{1/2} \tag{4.6}$$

The exponential factor, $\exp(-(c/2)|(\partial S/\partial \mathbf{x})|^2)$, which can be used for Monte Carlo importance sampling, favors the regions of space near the points of stationary phase (which are determined by $(\partial S/\partial \mathbf{x}) = 0$). In the limit that the parameter $c \to \infty$, eq 4.6 in fact yields the stationary phase approximation to the integral

$$I_{\text{SPA}} = \sum_k A(\mathbf{x}_k)\, e^{iS(\mathbf{x}_k)} \left[(2\pi i)^F \middle/ \left| \frac{\partial^2 S}{\partial \mathbf{x}\,\partial \mathbf{x}} \right| \right]^{1/2} \tag{4.7}$$

where F is the dimension of the integral and $\{\mathbf{x}_k\}$ the points of stationary phase. In the limit $c = 0$, eq 4.6 reverts to the original integral, eq 4.5, but with poor Monte Carlo statistics. The strategy is thus to evaluate eq 4.6 for finite c, extrapolating to values small enough that the c ≈ 0 limit can be determined.

V. Applications to Complex Systems; Time Correlation Functions

To deal with molecular processes for truly complex systems, e.g., chemical reactions, molecular energy transfer, photodissociation (or detachment) in clusters, liquids, solids, proteins, etc., it is useful to focus directly on the time correlation function relevant to the quantity of interest. These are of the form[16]

$$C_{AB}(t) = \text{tr}[\hat{A}\, e^{i\hat{H}t/\hbar}\hat{B}\, e^{-i\hat{H}t/\hbar}] \tag{5.1}$$

where operator $\hat{A}$ typically involves all the degrees of freedom of the molecular system (e.g., it usually involves the Boltzmann operator $e^{-\beta\hat{H}}$), $\hat{H}$ is the Hamiltonian of the complete molecular system, but $\hat{B}$ typically involves only a few degrees of freedom (e.g., those of the solute). For example, the reactive flux correlation function,[38] the long time limit of which gives the rate constant for a chemical reaction, corresponds to eq 5.1, with operators $\hat{A}$ and $\hat{B}$ given by

$$\hat{A} = e^{-\beta\hat{H}/2}\, \hat{F}\, e^{-\beta\hat{H}/2} \tag{5.2a}$$

$$\hat{B} = h(s(\hat{\mathbf{q}})) \tag{5.2b}$$

where $\hat{F}$ is the flux operator

$$\hat{F} = \frac{i}{\hbar}[\hat{H}, h(s(\hat{\mathbf{q}}))] \tag{5.2c}$$

and $h(s(\hat{\mathbf{q}}))$ the Heaviside function that is 1(0) on the product (reactant) side of the "dividing surface", defined by $s(\mathbf{q}) = 0$, which separates reactants and products.

Straightforward use of the SC-IVR for each of the time evolution operators in eq 5.1 thus leads to a double phase space average,[15a]

$$C_{AB}(t) = \int d\mathbf{p}_0 \int d\mathbf{q}_0 \int d\mathbf{p}_0' \int d\mathbf{q}_0' \langle \mathbf{q}_0|\hat{A}|\mathbf{q}_0'\rangle \times$$
$$\langle \mathbf{q}_t'|\hat{B}|\mathbf{q}_t\rangle\, e^{i(S_t - S_t')/\hbar} \left|\frac{\partial \mathbf{q}_t}{\partial \mathbf{p}_0}\right|^{1/2} \left|\frac{\partial \mathbf{q}_t'}{\partial \mathbf{p}_0'}\right|^{1/2}/(2\pi\hbar)^F \tag{5.3}$$

where here the Van Vleck (coordinate space) IVR has been used, and coordinates and momenta for all degrees of freedom are denoted by $(\mathbf{q},\mathbf{p})$, with $\mathbf{q}_t = \mathbf{q}_t(\mathbf{p}_0,\mathbf{q}_0)$, $\mathbf{q}_t' = \mathbf{q}_t(\mathbf{p}_0',\mathbf{q}_0')$, $S_t = S_t(\mathbf{p}_0,\mathbf{q}_0)$, and $S_t' = S_t(\mathbf{p}_0',\mathbf{q}_0')$. The interference between the trajectories with different initial conditions is the source of computational difficulty, but it is also the source of the quantum effects, so one must deal it.

A. Linearization Approximation. An approximate way to deal with the oscillatory integrand in the double phase space average (eq 5.3) is to assume that the only important contribution comes when the two trajectories are infinitesimally close to one another. This (admittedly drastic!) approximation is implemented by changing integration variables from $(\mathbf{p}_0,\mathbf{q}_0)$ and $(\mathbf{p}_0',\mathbf{q}_0')$ to

$$\bar{\mathbf{p}}_0 = \frac{1}{2}(\mathbf{p}_0 + \mathbf{p}_0')$$
$$\Delta\mathbf{p}_0 = \mathbf{p}_0' - \mathbf{p}_0$$
$$\bar{\mathbf{q}}_0 = \frac{1}{2}(\mathbf{q}_0 + \mathbf{q}_0')$$
$$\Delta\mathbf{q}_0 = \mathbf{q}_0' - \mathbf{q}_0 \tag{5.4}$$

and expanding the magnitude and phase of the integrand to first order in $\Delta\mathbf{p}_0$ and $\Delta\mathbf{q}_0$; the result gives the classical Wigner approximation

$$C_{AB}(t) \cong (2\pi\hbar)^{-F} \int d\bar{\mathbf{p}}_0 \int d\bar{\mathbf{q}}_0\, A_w(\bar{\mathbf{p}}_0,\bar{\mathbf{q}}_0)B_w(\mathbf{p}_t,\mathbf{q}_t) \tag{5.5}$$

where $\mathbf{p}_t = \mathbf{p}_t(\bar{\mathbf{p}}_0,\bar{\mathbf{q}}_0)$, $\mathbf{q}_t = \mathbf{q}_t(\bar{\mathbf{p}}_0,\bar{\mathbf{q}}_0)$, and A_w and B_w are the Wigner functions[39] corresponding to these operators

$$A_w(\mathbf{p},\mathbf{q}) = \int d\mathbf{q}'\, e^{-i\mathbf{p}\mathbf{q}'/\hbar}\langle \mathbf{q} + \mathbf{q}'/2|\hat{A}|\mathbf{q} - \mathbf{q}'/2\rangle \tag{5.6}$$

and similarly for B_w. Equation 5.5, which we have referred to as the linearized approximation[10j] of the full SC-IVR expression (LSC-IVR), is thus effectively a classical calculation with the Wigner functions replacing the classical functions; i.e., if $A_w(\mathbf{p},\mathbf{q})$ and $B_w(\mathbf{p},\mathbf{q})$ were replaced by $A_{CL}(\mathbf{p},\mathbf{q})$ and $B_{CL}(\mathbf{p},\mathbf{q})$, respectively, then eq 5.5 becomes precisely the classical expression for the correlation function. The idea of carrying out an essentially classical calculation with Wigner functions has arisen many times in the past[40,15b] from different formulations; it is interesting here to see how it emerges as an approximation to the SC-IVR. (A similar kind of linearization
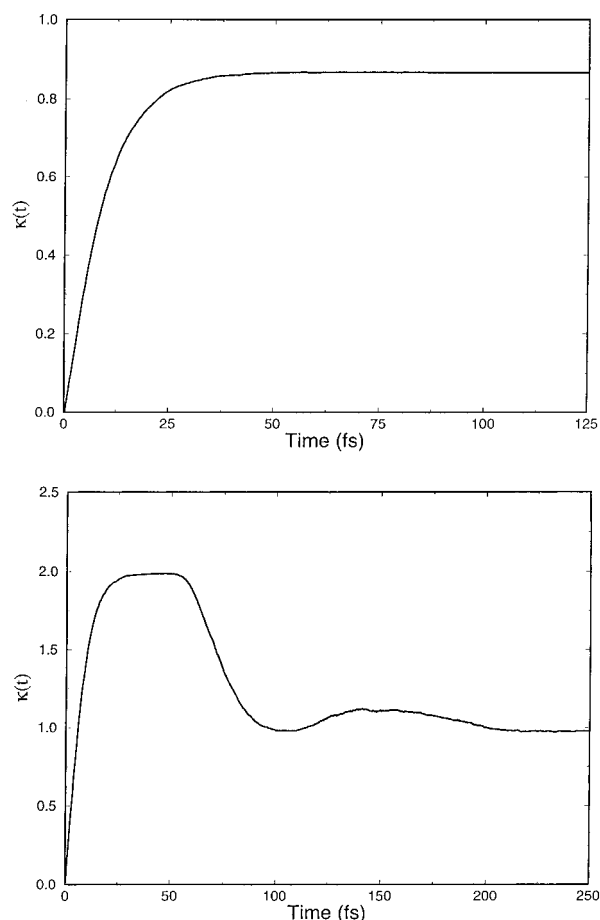
Figure 2. Reactive flux correlation function for a double well potential coupled to a bath of harmonic oscillators: (a) strong and (b) weak coupling to the bath, respectively; from ref 10j.

Figure 3. Decay of the population difference, $D(t) = P_1(t) - P_2(t)$, for a two-(electronic) state system coupled to a bath of harmonic oscillators (where state 1 is the initial state): (a) weak and (b) strong coupling to the bath; from ref 10l.

approximation was also used in the older SC framework to obtain dipole−dipole correlation functions for spectral line shapes.[5e])

Because the LSC-IVR/classical Wigner model is so simple, it has been applied to several benchmark model problems to illustrate what it can and cannot do. Figure 2, for example, shows the flux correlation function (cf. eq 5.2) for a model of an isomerization reaction in a condensed phase medium, namely, a double-well potential coupled to a bath of harmonic oscillators.[10j] Figure 2a is for the case of strong coupling to the bath, for which there is no recrossing flux (and therefore for which transition state theory (TST) is a good approximation), and Figure 2b is for the case of weak coupling. In the latter case, flux recrosses the dividing surface several times before the products are thermalized; TST is of course not valid in this regime. The rate constants (the long time limit of the correlation function) given by the LSC-IVR/classical Wigner model are in excellent agreement with accurate quantum results in both of these regimes.

Figure 3 shows an example using the classical model of electronically nonadiabatic processes summarized in section III.[10l] It is a model of an electron-transfer reaction (or any other "radiationless transition") in a condensed phase, specifically a two-state system coupled to a harmonic bath (often referred to as the "spin-boson" model). Figure 3a shows the population relaxation for weak coupling to the bath so that the population hops back and forth a number of times before thermalization, and Figure 3b shows the case of strong coupling, for which these oscillations do not occur because the system is thermalized
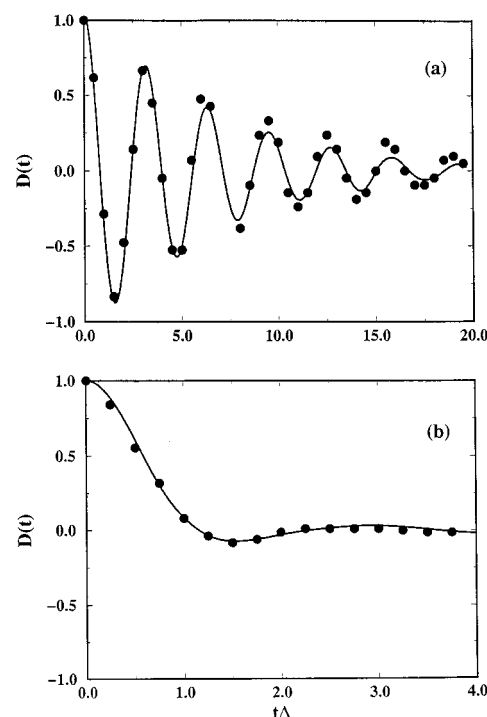
too quickly. Again, the LSC-IVR/classical Wigner approximation gives results in very good agreement with the correct quantum results (also shown in Figure 3).

The LSC-IVR/classical Wigner model thus works quite well for these examples, and there should be many realistic molecular systems for which it does a good job. Unfortunately, though, a more detailed analysis[10k] shows that it cannot describe quantum coherence effects (there can also be coherent motion classically, which it does of course describe correctly). An application of the LSC-IVR to inelastic scattering,[10o] for example, showed it to give a poor description of interference effects in the product state distribution (while the full SC-IVR treatment describes them extremely well). Use of the Wigner function for the Boltzmannized flux operator (cf. Eq(5.2a)) does incorporate some quantum effects in the flux correlation function: specifically, the quantum behavior is described well for short time, $t < \hbar\beta$; the longer-time behavior, however, is strictly that given by classical mechanics. (Quantum effects in the long time dynamics were thus not important for the two examples discussed above,[10j,10l] but this is not always the case (vide infra).) Because it describes the short time quantum behavior well, the LSC-IVR/classical Wigner model can serve as the basis for a quantum transition state theory (because TST is based on the short time behavior of the flux correlation function); Pollak et al.[41] have pursued idea this quite fruitfully.

B. Forward−Backward IVR. To go beyond the linearized SC-IVR or classical Wigner approximation, yet avoid having to deal with the double phase space average in eq 5.3, we have utilized an idea suggested by some interesting work of Thompson and Makri,[42a,b] namely, to combine the two propagators $e^{-i\hat{H}t/\hbar}$, which propagates from 0 to t, and $e^{+i\hat{H}t/\hbar}$, which propages from t to 0, into one semiclassical propagation from 0 to 0; i.e., since the SC-IVR makes the semiclassical approximation from 0 to t and from t to 0, one might as well also make it *at* time t and have just a single SC-IVR for the Heisenberg operator

$$\hat{B}^H(t) \equiv e^{i\hat{H}t/\hbar}\hat{B}\,e^{-i\hat{H}t/\hbar} \tag{5.7}$$

The complicating feature, of course, is that operator $\hat{B}$ stands between the forward and the backward propagators in eq 5.7, so that one must learn how to deal with it semiclassically. (Thompson and Makri used the forward−backward[42a,b] idea to construct an influence functional (semiclassically) for an anharmonic "bath" coupled to a quantum "system". The above "complicating feature" does not arise in this case because the propagators in the influence functional involve only the bath degrees of freedom and operator $\hat{B}$ only those of the system).

The key idea[10m,q] is to write operator $\hat{B}$ as an intergral transform of an exponential operator, for which a semiclassical treatment is straightforward. For the reactive flux correlation function, for example, operator $\hat{B}$ is

$$\hat{B} = h[s(\hat{\mathbf{q}})] \tag{5.8a}$$

since it is a function of coordinates only through the one collective variable $s(\mathbf{q})$, the appropriate integral transform is a 1-d Fourier transform

$$\hat{B} = \int_{-\infty}^{\infty} dp_s\, \tilde{B}(p_s)\, e^{ip_s s(\hat{\mathbf{q}})/\hbar} \tag{5.8b}$$

where

$$\tilde{B}(p_s) = \lim_{\epsilon \to 0}[2\pi i(p_s - i\epsilon)]^{-1} \tag{5.8c}$$

(In practice one can set $\epsilon = 0$ since the other factors in the integrand are zero for $p_s = 0$.) The coherent state IVR is then used for the product of operators

$$e^{i\hat{H}t/\hbar}\, e^{ip_s s(\hat{\mathbf{q}})/\hbar}\, e^{-i\hat{H}t/\hbar}$$

which can be thought of as three successive propagators. The result (which can be derived in several ways[10m,q,u]) has the standard Herman−Kluk form of eq 2.11

$$e^{i\hat{H}t/\hbar}\, e^{ip_s s(\hat{\mathbf{q}})/\hbar}\, e^{-i\hat{H}t/\hbar} = (2\pi\hbar)^{-F}\int d\mathbf{p}_0 \int$$
$$d\mathbf{q}_0\, C_0(\mathbf{q}_0,\mathbf{p}_0;p_s)\, e^{iS_0(\mathbf{q}_0,\mathbf{p}_0;p_s)/\hbar}|\mathbf{p}_0',\mathbf{q}_0'\rangle\langle\mathbf{p}_0,\mathbf{q}_0| \tag{5.9a}$$

where $(\mathbf{q}_0',\mathbf{p}_0')$ are the final coordinates and momenta that result from the trajectory which begins at $t = 0$ with initial conditions $(\mathbf{q}_0,\mathbf{p}_0)$, evolves via the full (classical) Hamiltonian H until time t—yielding coordinates and momenta $(\mathbf{q}_t,\mathbf{p}_t)$—then has the momenta changed according to

$$\mathbf{p}_t \to \mathbf{p}_t + p_s\frac{\partial s(\mathbf{q}_t)}{\partial\mathbf{q}_t} \tag{5.9b}$$

and is then propagated backward in time to $t = 0$. The action integral S_0 is

$$S_0(\mathbf{p}_0,\mathbf{q}_0) = \int_0^t dt'\,(\mathbf{p}_t\dot{\mathbf{q}}_t - \mathbf{H}) + p_s s(\mathbf{q}_t) + \int_t^0 dt'\,(\mathbf{p}_t\dot{\mathbf{q}}_t - \mathbf{H}) \tag{5.9c}$$

and the HK prefactor C_0 involves the same derivatives of final values with respect to initial ones as in eq 2.11b.

With the intergral transform for operator $\hat{B}$ (eq 5.8b) and the FB-IVR for the product of exponential operators (eq 5.9), the reactive flux correlation function—or any correlation function with operator $\hat{B}$ of the form $B(s(\hat{\mathbf{q}}))$—is given by

$$C_{AB}(t) = \int_{-\infty}^{\infty} dp_s\, \tilde{B}(p_s)(2\pi\hbar)^{-F}\int d\mathbf{p}_0 \int$$
$$d\mathbf{q}_0\, C_0(\mathbf{p}_0,\mathbf{q}_0;p_s)\, e^{iS_0(\mathbf{p}_0,\mathbf{q}_0;p_s)/\hbar}\langle\mathbf{p}_0,\mathbf{q}_0|\hat{A}|\mathbf{p}_0',\mathbf{q}_0'\rangle \tag{5.10}$$

There is thus a *single* phase space integral over all degrees of freedom—the same level of complexity as for a completely classical calculation—plus a one-dimensional integral over the "jump" parameter p_s, which is the magnitude of the momentum jump at time t. It is hard to imagine anything simpler than this that is capable (see below) of describing true quantum coherence features. Note also that the direction of the momentum jump is a normal to the dividing surface defined by $s(\mathbf{q}) = 0$; thus, in a complex molecular system—e.g., a liquid, a protein, etc.—the (many) degrees of freedom that are not directly coupled to the reaction coordinate will experience no momentum jump at time t and thus—to the extent that they are not coupled to the reaction coordinate motion—back-integrate in the backward step $t \to 0$. Their contribution to the net action S_0, eq 5.9c, will thus cancel out; only the reaction coordinate and those degrees of freedom significantly coupled to it contribute to the action. This self-cancellation of the oscillatory character of the integrand induced by the combined forward−backward trajectory is its most important feature. More general operators $\hat{B}$, i.e., those that involve momentum as well as coordinate operators, can be treated by a generalization[10q] of the above Fourier transform (the Weyl-ordered product representation).

It is also easy to see what approximation to eq 5.10 causes it to revert to the essentially classical result: if one assumes that only small values of p_s contribute to the integral over it, then one can make a first-order cumulant approximation to the p_s dependence of the integrand

$$\langle\mathbf{p}_0,\mathbf{q}_0|\hat{A}|\mathbf{p}_0',\mathbf{q}_0'\rangle C_0(\mathbf{p}_0,\mathbf{q}_0;\mathbf{p}_s)\, e^{iS_0(\mathbf{p}_0,\mathbf{q}_0;\mathbf{p}_s)/\hbar} \cong$$
$$\langle\mathbf{p}_0,\mathbf{q}_0|\hat{A}|\mathbf{p}_0,\mathbf{q}_0\rangle\, e^{ip_s a_t(\mathbf{p}_0,\mathbf{q}_0)/\hbar} \tag{5.11}$$

(since $C_0(\mathbf{p}_0,\mathbf{q}_0;0) = 1$, $S_0(\mathbf{p}_0,\mathbf{q}_0;0) = 0$). The diagonal coherent-state matrix element of an operator is its Husimi function[43]

$$A_H(\mathbf{p}_0,\mathbf{q}_0) \equiv \langle\mathbf{p}_0,\mathbf{q}_0|\hat{A}|\mathbf{p}_0,\mathbf{q}_0\rangle \tag{5.12}$$

which is similar (though not identical) to the Wigner function, and the parameter $a_t(\mathbf{p}_0,\mathbf{q}_0)$ is essentially the classically evolved function $s_t(\mathbf{p}_0,\mathbf{q}_0)$; bringing the $\int dp_s$ inside the phase space average thus inverts the Fourier transform $\tilde{B}(p_s)$, to give

$$C_{AB}(t) \cong (2\pi\hbar)^{-F}\int d\mathbf{p}_0 \int d\mathbf{q}_0\, A_H(\mathbf{p}_0,\mathbf{q}_0)B(s_t(\mathbf{q}_0,\mathbf{p}_0)) \tag{5.13}$$

which one might call the classical Husimi model; it has the same form as the classical Wigner model of eq 5.5 but with Husimi functions (Husimi functions arise naturally in a coherent-state representation, and Wigner functions in a coordinate-space representation), and is also seen to arise from making a linearization approximation, here a linearization of the integrand in the jump parameter p_s.

Finally, we note that there is another way of implementing the forward−backward idea for the complete molecular system: the Heisenberg time evolved operator $\hat{B}$ of eq 5.7 can also be written as

$$\hat{B}^H(t) \equiv e^{i\hat{H}t/\hbar}\hat{B}\,e^{-i\hat{H}t/\hbar} = -i\frac{d}{d\lambda}e^{i\hat{H}t/\hbar}\,e^{i\lambda\hat{B}}\,e^{-i\hat{H}t/\hbar},\ \lambda = 0 \tag{5.14a}$$

and the above forward−backward SC-IVR used to obtain the product of exponential operators

$$e^{i\hat{H}t/\hbar}\, e^{i\lambda\hat{B}}\, e^{-i\hat{H}t/\hbar} \qquad (5.14b)$$

just as above, leading to a momentum jump (if $\hat{B} = B(s(\hat{\mathbf{q}}))$ at time t given by

$$\mathbf{p}_t \rightarrow \mathbf{p}_t + \lambda B'(s(\mathbf{q}_t))\, \frac{\partial s(\mathbf{q}_t)}{\partial \mathbf{q}_t} \qquad (5.15)$$

Sun and Miller[10q] tried this derivative form of the Heisenberg operator, and Makri et al.[42] have pursued it more fully. The problem is that since λ is infinitesimal (and ultimately set to zero), the momentum jump at time t vanishes so that the backward trajectory exactly retraces the forward trajectory. There is thus no possibility of interference effects between distinct trajectories, very much the same shortcoming as that of the linearized (classical Wigner) approximation. The effective equivalence of the derivative form of the FB-IVR and the linearized approximation has been seen in applications[42d] and can also be shown algebraically. Thus, if one explicitly differentiates the λ-dependence of the FB-IVR expression for the quantity in eq 5.14 and then sets λ to zero, the following expression for the correlation function is obtained

$$C_{AB}(t) = (2\pi\hbar)^{-F}\!\int d\mathbf{p}_0 \int d\mathbf{q}_0\, B(s(\mathbf{q}_t))\Bigg[1 - \frac{1}{4}\Bigg(\gamma\hbar^2\, \frac{\partial^2}{\partial \mathbf{p}_0^{\,2}} +$$
$$\frac{1}{\gamma}\, \frac{\partial^2}{\partial \mathbf{q}_0^{\,2}}\Bigg)\Bigg]A_{H}(\mathbf{p}_0,\mathbf{q}_0) \quad (5.16)$$

where A_{H} is the Husimi function (eq 5.12). Noting the relation between the Wigner and Husimi distributions

$$A_{w}(\mathbf{p}_0,\mathbf{q}_0) = \exp\Bigg[-\frac{1}{4}\Bigg(\gamma\hbar^2\, \frac{\partial^2}{\partial \mathbf{p}_0^{\,2}} + \frac{1}{\gamma}\, \frac{\partial^2}{\partial \mathbf{q}_0^{\,2}}\Bigg)\Bigg]A_{H}(\mathbf{p}_0,\mathbf{q}_0) \quad (5.17)$$

one sees that eq 5.16 is indeed approximately the same as the classical Wigner (linearized) model

$$C_{AB}^{Wigner}(t) \equiv (2\pi\hbar)^{-F}\!\int d\mathbf{p}_0 \int d\mathbf{q}_0\, B(s(\mathbf{q}_t))A_{w}(\mathbf{p}_0,\mathbf{q}_0) \quad (5.18)$$

C. Applications of the FB-IVR. The form of the FB-IVR for the correlation function suggests a natural way to proceed with a calculation. For example, for operators $\hat{B}$ of the form $B(s(\hat{\mathbf{q}}))$, eq 5.10 for the correlation function can be written as

$$C_{AB}(t) = \int_{-\infty}^{\infty} dp_s\, \tilde{B}(p_s)(2\pi\hbar)^{-F}\!\int d\mathbf{p}_0 \int d\mathbf{q}_0\, A_{H}(\mathbf{p}_0,\mathbf{q}_0) \times$$
$$\{C_0(\mathbf{p}_0,\mathbf{q}_0;p_s)\, e^{iS_0(\mathbf{p}_0,\mathbf{q}_0;p_s)/\hbar}\, \langle\mathbf{p}_0,\mathbf{q}_0|\hat{A}|\mathbf{p}_0',\mathbf{q}_0'\rangle/\langle\mathbf{p}_0,\mathbf{q}_0|\hat{A}|\mathbf{p}_0,\mathbf{q}_0\rangle\} \quad (5.19)$$

where $A_{H}(\mathbf{p}_0,\mathbf{q}_0)$ is the Husimi distribution function corresponding to operator $\hat{A}$. The Husimi distribution provides the natural weighting function for a Monte Carlo average over initial conditions. FB-IVR calculations have been carried out this way for the reactive flux correlation function for a system consisting of a one-dimensional double well potential coupled to up to 40 vibrational degrees of freedom,[10u] with excellent agreement with essentially exact quantum (path integral) calculations for this system. A full-dimensional treatment of hydrogen atom transfer in hydroxyphenyl oxazole[10x] (51 vibrational degrees of freedom) has also been successfully treated this way. It has also been applied to the femtosecond photodetachment of I_2^- (which involves the evaluation of optical response functions by the FB-IVR)[10p] and also to molecular energy transfer distribution functions[10t] (i.e., $P(E'\leftarrow E)$). There is also a recent very suc-
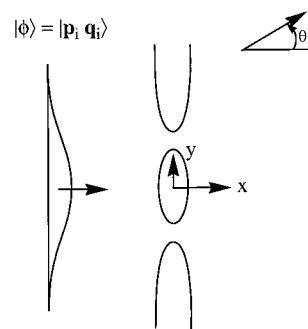

Figure 4. Contour sketch of the two-slit potential energy surface, $V(x,y)$, with the initial state $|\phi\rangle$ depicted; from ref 10y.

cessful FB-IVR calculation by Ovchinnikov et al.[15c] of the resonance Raman spectrum of I_2 in a cluster of up to 10 Xenon atoms.

To have a simple example, however, that can clearly distinguish between which theoretical approaches can, and cannot, describe true quantum coherence effects, we have considered the textbook paradigm of quantum coherence phenomena, namely transmission through a "two-slit" potential.[10y] Figure 4 shows the sketch of a contour plot of the 2-d potential energy surface $V(x,y)$ for this scattering problem. The initial state $\phi(\mathbf{q})[\mathbf{q}=(x,y)]$ is a coherent state

$$|\phi\rangle = |\mathbf{p}_i\mathbf{q}_i\rangle \qquad (5.20)$$

with $\mathbf{q}_i$ localized in the region to the left of the barrier ($x < 0$) and momentum $\mathbf{p}_i$ in the x-direction. What is calculated is the probability $P(\theta)$ of the particle emerging to the right side of the barrier ($x > 0$) at angle θ. With operators $\hat{A}$ and $\hat{B}$ defined by

$$\hat{A} = |\phi\rangle\langle\phi| \qquad (5.21a)$$
$$\hat{B} = \delta((\theta - \theta(\hat{\mathbf{q}})) \qquad (5.21b)$$

the correlation for $C_{AB}(t\rightarrow\infty)$ is $P(\theta)$

$$P(\theta) = \langle\phi|e^{i\hat{H}t/\hbar}\delta((\theta - \theta(\hat{\mathbf{q}}))\, e^{-i\hat{H}t/\hbar}|\phi\rangle) \qquad (5.22a)$$
$$= (2\pi\hbar)^{-1}\int_{-\infty}^{\infty} dp_\theta\, e^{-ip_\theta\theta/\hbar}\langle\phi|e^{i\hat{H}t/\hbar}\, e^{ip_\theta\theta(\hat{\mathbf{q}})/\hbar}\, e^{-i\hat{H}t/\hbar}|\phi\rangle \qquad (5.22b)$$

and the limit of large t is taken. The FB-IVR is used to evaluate the matrix element in eq 5.22b, and the general expression (eq 5.19) in this case becomes

$$P(\theta) = (2\pi\hbar)^{-1}\!\int dp_\theta\, e^{-ip_\theta\theta/\hbar}\!\int d\mathbf{p}_0 \int d\mathbf{q}_0\, \rho_{H}(\mathbf{p}_0,\mathbf{q}_0)$$
$$\left\{\frac{\langle\phi|\mathbf{p}_0',\mathbf{q}_0'\rangle}{\langle\phi|\mathbf{p}_0,\mathbf{q}_0\rangle}C_0(\mathbf{p}_0,\mathbf{q}_0;p_\theta)\, e^{iS_0(\mathbf{p}_0,\mathbf{q}_0;p_\theta)/\hbar}\right\} \quad (5.23a)$$

where ρ_{H} is the (normalized) Husimi distribution function corresponding to the initial state

$$\rho_{H}(\mathbf{p}_0,\mathbf{q}_0) = (2\pi\hbar)^{-F}|\langle\mathbf{p}_0,\mathbf{q}_0|\phi\rangle|^2 = (2\pi\hbar)^{-F}|\langle\mathbf{p}_0,\mathbf{q}_0|\mathbf{p}_i,\mathbf{q}_i\rangle|^2$$
$$= (2\pi\hbar)^{-F}\exp\Bigg[\frac{-\gamma}{2}(\mathbf{q}_0 - \mathbf{q}_i)^2 - (\mathbf{p}_0 - \mathbf{p}_i)^2/2\hbar^2\gamma\Bigg] \quad (5.23b)$$

One thus performs a Monte Carlo average of the quantity in curly brackets in eq 5.23a using the Husimi distribution of eq 5.23b as the sampling function.
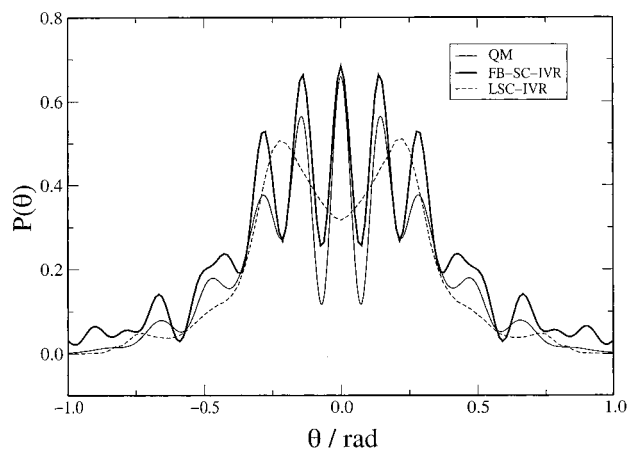
Feature Article

J. Phys. Chem. A, Vol. 105, No. 13, 2001 **2951**

Figure 5. Angular distribution of a particle transmitted through the two-slit potential, as given by the exact quantum calculation (QM), the forward−backward IVR (eq 5.23a) (FB−SC-IVR), and the linearized/classical Wigner model (LSC-IVR); from ref 10y.

Figure 6. Same as Figure 5, but with the addition of a bath of harmonic oscillators coupled to the two-slit potential; the different curves are for different temperatures for the harmonic bath; from ref 10y.

Figure 5 shows $P(\theta)$ given by the FB-IVR, compared to the exact quantum result and also the result of the LSC-IVR/Wigner model. One sees that the latter approximation is not able to describe the interference structure (i.e., diffraction) while the FB-IVR can do so, and the reason is rather obvious: the LSC-IVR implicitly assumes that the forward and backward trajectories are infinitesimally close to each other (the same as the small p_θ approximation), so there is only a contribution from a trajectory that goes through one of the holes and comes back through the same hole. (Note that the final phase point $(\mathbf{p}_0', \mathbf{q}_0')$, as well as the initial one $(\mathbf{p}_0, \mathbf{q}_0)$, must not be too far from $(\mathbf{p}_i, \mathbf{q}_i)$; cf. eq 5.23b.) The FB-IVR, however, integrates over all values of the jump parameter so that some trajectories that go through one of the holes make the appropriate jump (at time t) to come back through the other hole (and overlap the initial state). The classical Wigner or Husimi (i.e., linearized) approximations can never describe this effect, which is the hallmark of semiclassical theory (i.e., interference between different classical trajectories).

This example becomes even more interesting when a harmonic bath is introduced that is coupled to the y-degree of freedom; i.e., the two slits are "jiggled" vertically in Figure 4 by interaction with these degrees of freedom. Operator $\hat{A}$ then becomes

$$\hat{A} = Z^{-1} e^{-\beta \hat{H}_b} |\phi\rangle\langle\phi| \qquad (5.24a)$$

where $\hat{H}_b$ is the Hamiltonian of the harmonic bath and $Z = \text{tr}(e^{-\beta \hat{H}_b})$. Equation 5.23a then generalizes to

$$P(\theta) = (2\pi\hbar)^{-1} \int d p_\theta \, e^{-i p_\theta \theta/\hbar} \int d\mathbf{p}_0 \int d\mathbf{q}_0 \int d\mathbf{P}_0 \int d\mathbf{Q}_0$$

$$\rho_H(\mathbf{p}_0,\mathbf{q}_0,\mathbf{P}_0,\mathbf{Q}_0) \left\{ \frac{\langle\phi|\mathbf{p}_0',\mathbf{q}_0'\rangle}{\langle\phi|\mathbf{p}_0,\mathbf{q}_0\rangle} \frac{\langle\mathbf{P}_0,\mathbf{Q}_0|e^{-\beta \hat{H}_b}|\mathbf{P}_0',\mathbf{Q}_0'\rangle}{\langle\mathbf{P}_0,\mathbf{Q}_0|e^{-\beta \hat{H}_b}|\mathbf{P}_0,\mathbf{Q}_0\rangle} C_0 \, e^{iS_0/\hbar} \right\}$$

$$(5.24b)$$

where

$$\rho_H(\mathbf{p}_0,\mathbf{q}_0,\mathbf{P}_0,\mathbf{Q}_0) =$$
$$(2\pi\hbar)^{-F} |\langle\mathbf{p}_0,\mathbf{q}_0|\phi\rangle|^2 \langle\mathbf{P}_0,\mathbf{Q}_0|e^{-\beta \hat{H}_b}|\mathbf{P}_0,\mathbf{Q}_0\rangle/Z \quad (5.24c)$$

Figure 6 shows $P(\theta)$ so calculated[10y] for various values of the bath temperature. As expected, as the temperature of the bath is increased, the interference is progressively quenched. T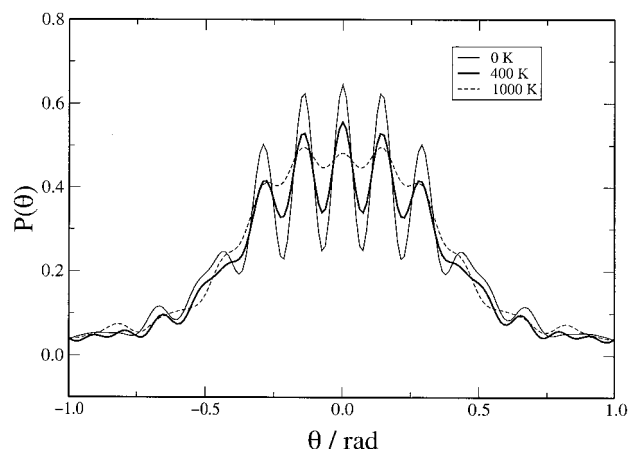his is an example of the popularly discussed phenomenon of "decoherence" caused by coupling to an "environment", but it is no different from many earlier examples of quenching[44,45] of interference features when some degrees of freedom (here the harmonic bath) are averaged over.

The important thing is that the FB-IVR is able to describe true quantum interference phenomena (and its quenching)! And the calculation is not so much more difficult than a completely classical one; i.e., in both, one must average over the phase space of initial conditions, and in the FB-IVR, one must also integrate over a one-dimensional (in these examples) jump parameter.

Another dramatic illustration of the ability of the FB-IVR to describe quantum coherence effects is provided by considering the time-dependent probability distribution of a vibrational coordinate (i.e., a diatomic molecule) in a condensed phase environment (e.g., a liquid, a cluster, etc.), modeled here again by the ubiquitous harmonic bath.[10z] The quantity of interest is $P_t(r)$

$$P_t(r) = \text{tr}[\hat{A} \, e^{i\hat{H}t/\hbar} \delta(r - r(\hat{\mathbf{q}})) \, e^{-i\hat{H}t/\hbar}] \qquad (5.25a)$$

which (analogous to $P(\theta)$ above) corresponds to the correlation function $C(t)$ with

$$\hat{A} = |\phi\rangle\langle\phi| \, e^{-\beta \hat{H}_b}/Z \qquad (5.25b)$$

$$\hat{B} = \delta(r - r(\hat{\mathbf{q}})) \qquad (5.25c)$$

(Note that $P_t(r)$ would simply be the square modulus of the time-dependent wave function, $|\psi(r,t)|^2$, for an isolated diatomic molecule.) With the delta function, eq 5.26c, represented in the usual way

$$\delta(r - r(\hat{\mathbf{q}})) = (2\pi\hbar)^{-1} \int_{-\infty}^{\infty} d p_r \, e^{-p_r r/\hbar} e^{i p_r r(\hat{\mathbf{q}})/\hbar} \quad (5.26)$$

the result for the distribution function $P_t(r)$ is the same as eq 5.24 (with $\theta \rightarrow r$, $p_\theta \rightarrow p_r$, etc.).

Figure 7 shows $P_t(r)$ first for the diatomic (a Morse potential with parameters corresponding to I$_2$, for which the vibrational period is ~156 fsec) uncoupled to the harmonic bath. (The initial state $|\phi\rangle$ for the diatomic is a coherent state $|p_i,q_i\rangle$, with $p_i = 0$ and $q_i = 2.4$ Å, considerably compressed from its equilibrium value $r_{eq} = 2.67$ Å.) Figure 7a is for $t = 192$ fsec (about 1.2 vibrational periods), Figure 7b for $t = 640$ fsec (about 4 vibrational periods), and Figure 7c for $t = 1600$ fsec (about 10 vibrational periods); in each case, the FB-IVR result is the
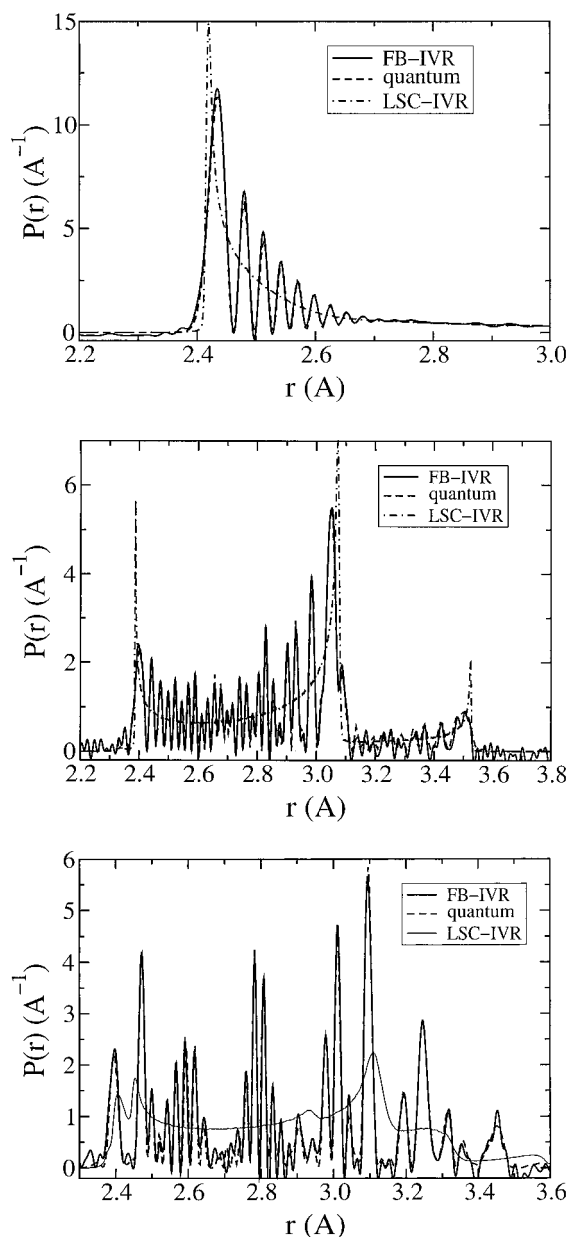
Figure 7. Probability distribution of the vibrational coordinate of a diatomic molecule (a Morse potential with parameters corresponding to I_2): (a)$t = 192$, (b) 640, and (c) 1600 fsec; for comparison, the vibrational period is 156 fsec. The broken line is the exact quantum result (quantum), the heavy solid line the forward−backward IVR result (FB-IVR), and the thin solid line the linearized IVR/classical Wigner result (LSC-IVR); from ref 10z.

Figure 8. Same as Figure 7, but with the addition of a bath of harmonic oscillators, for $t = 192$ fsec; panels a−c are for the bath temperature as indicated. The solid line is the FB-IVR result, and the broken line the linearized IVR/classical Wigner (LSC-IVR) result.

Figure 9. Average position as a function of time t, for a particle in an anharmonic potential. The QM curve is the exact quantum result, and those labeled by the parameter c are for the Filinov parameters $c_1 = c_2 = c$ of eqs 6.6−6.8. $c = 0$ corresponds to the full SC-IVR (i.e., the double phase space average alá eq 6.2), and the FB-IVR result corresponds to $c = \infty$ (i.e., the single phase space average alá eq 6.4).

solid curve, the exact QM result the dashed line, and the LSC-IVR/classical Wigner result the dash-dot line. One sees a great deal of quantum coherence structure—because many vibrational states are mixed in by this initial state—and that the FB-IVR describes it essentially quantitatively, while (as expected) the linearized/Wigner approximation (i.e., classical mechanics with a Wigner distribution of initial conditions) has no hint of it.

Figure 8 now shows how this is modified by coupling to a bath (modeled by 40 explicit harmonic modes) at various temperatures.[10z] At sufficiently high temperature (depending on the strength of the coupling), the interference structure is quenched, and in this limit the FB-IVR results are essentially the same as the classical Wigner model. Thus again, the FB-IVR is able to describe the quantum interference structure
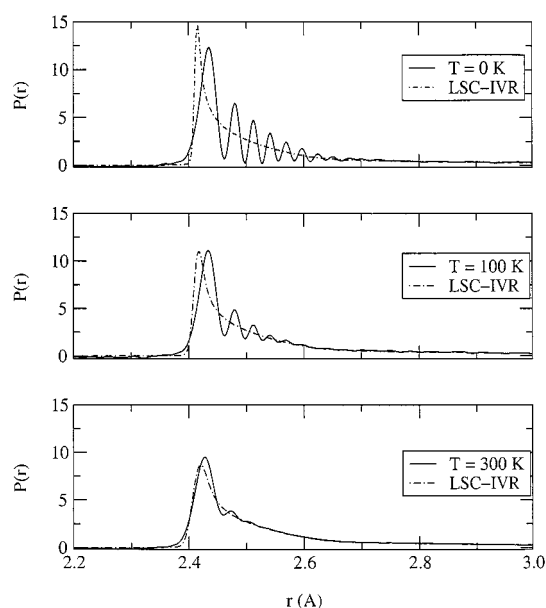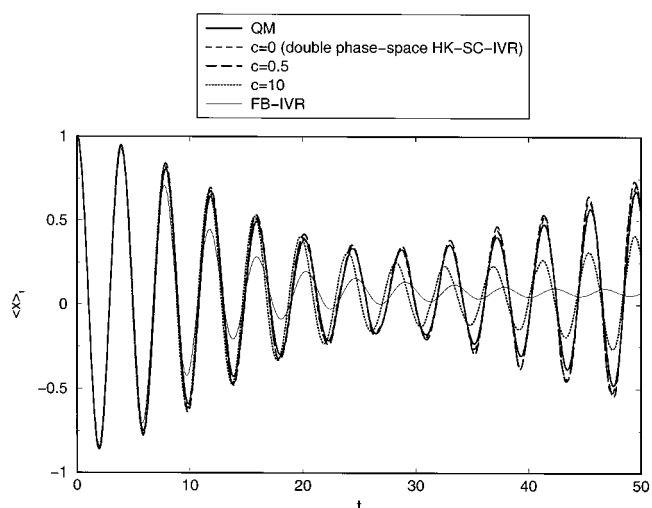
extremely well, and also the quenching ("decoherence") that is induced by coupling to degrees of freedom that are averaged over.

VI. Further Improvements

Finally, as impressive as the performance of the FB-IVR of the previous section is, there are some situations for which it is inadequate. Figure 9, for example, shows an example used by Makri, et al.,[42d] the expectation value of $\hat{x}$ in an 1-d anharmonic potential $V(x) = (^1/_2)c_2x^2 - c_3x^3 + c_4x^4$. (One can think of $\langle x \rangle_t$ as the correlation function $C_{AB}(t)$ with $\hat{A} = |\phi\rangle\langle\phi|$ and $\hat{B} = \hat{x}$.) The FB-IVR (the thin solid line in Figure 9) does not show the correct (thick solid line) recurrence of interference at longer time, i.e., after ∼10 vibrational periods. In this case, the FB-IVR gives essentially the same results as those of the linearized/

Feature Article

J. Phys. Chem. A, Vol. 105, No. 13, 2001 **2953**

classical Wigner approximation. The full HK, i.e., the double phase space average (eq 5.3), on the other hand (the curve labeled $c = 0$ in Figure 4), gives results essentially indistinguishable from those of the correct QM curve. One would thus like a way to go beyond the FB-IVR, but perhaps not all the way back to the full double phase space average of eq 5.3.

To see how to proceed, consider the product of two time evolution operators

$$\hat{K} = e^{-i\hat{H}_2/\hbar} e^{-i\hat{H}t_1/\hbar} \qquad (6.1)$$

(For the correlation function C_{AB}, $t_2 = -t_1$, and operator $\hat{B}$ stands between the two propagators, but this will be treated as before, so it is sufficient to consider the simpler quantity in eq 6.1.) If one uses a separate IVR, i.e., eq 2.11, for each propagator, then one obtains the following double phase space average

$$\hat{K} = (2\pi\hbar)^{-F}\int d\mathbf{p}_0 \int d\mathbf{q}_0 \, (2\pi\hbar)^{-F}\int d\mathbf{p}_1' \int d\mathbf{q}_1' \, |\mathbf{p}_2,\mathbf{q}_2\rangle \times$$
$$\langle\mathbf{p}_1',\mathbf{q}_1'|\mathbf{p}_1,\mathbf{q}_1\rangle\langle\mathbf{p}_0,\mathbf{q}_0|C_{t_1}(\mathbf{p}_0,\mathbf{q}_0)C_{t_2}(\mathbf{p}_1',\mathbf{q}_1')|e^{iS_{t_2}(\mathbf{p}_1',\mathbf{q}_1')/\hbar}$$
$$e^{iS_{t_1}(\mathbf{p}_0,\mathbf{q}_0)/\hbar} \qquad (6.2)$$

the notation here should be clear: e.g., $\mathbf{p}_1$, $\mathbf{q}_1 = \mathbf{p}_1(\mathbf{p}_0,\mathbf{q}_0)$, $\mathbf{q}_1$-$(\mathbf{p}_0,\mathbf{q}_0)$ are the variables at time t_1 that result from initial conditions $(\mathbf{p}_0,\mathbf{q}_0)$, and $\mathbf{p}_2$, $\mathbf{q}_2 = \mathbf{p}_2(\mathbf{p}_1',\mathbf{q}_1')$, $\mathbf{q}_2(\mathbf{p}_1',\mathbf{q}_1')$ are the values at time t_2 that result from $(\mathbf{p}_1',\mathbf{q}_1')$. On the other hand, one can clearly combine the two propagators in eq 6.1 into one propagator for time $(t_1 + t_2)$ (cf. the FB-IVR)

$$\hat{K} = e^{-i\hat{H}(t_2+t_1)/\hbar} \qquad (6.3)$$

and represent it via a single IVR

$$\hat{K} =$$
$$(2\pi\hbar)^{-F}\int d\mathbf{p}_0 \int d\mathbf{q}_0 \, |\mathbf{p}_2,\mathbf{q}_2\rangle\langle\mathbf{p}_0,\mathbf{q}_0|C_{t_1+t_2}(\mathbf{p}_0,\mathbf{q}_0) \, e^{iS_{t_1+t_2}(\mathbf{p}_0,\mathbf{q}_0)/\hbar}$$
$$(6.4)$$

where here $\mathbf{p}_2$, $\mathbf{q}_2 = \mathbf{p}_2(\mathbf{p}_0,\mathbf{q}_0)$, $\mathbf{q}_2(\mathbf{p}_0,\mathbf{q}_0)$ are the final values that evolve for time $(t_1 + t_2)$ from initial conditions $(\mathbf{p}_0,\mathbf{q}_0)$. What we wish to show is how to go continuously from the double IVR, eq 6.2, to the single IVR, eq 6.4.

The trick is to use the modified Filinov filtering scheme[37b] (cf. eq 4.6) applied to the double IVR, eq 6.2. The calculation is rather tedious but can be carried through; the $F = 1$ result is[10aa]

$$\hat{K} = (2\pi\hbar)^{-1}\int dp_0 \int dq_0 \, (2\pi\hbar)^{-1}\int dp_1' \int dq_1'$$
$$e^{iS_{t_2}(p_1',q_1')/\hbar} \, e^{iS_{t_1}(p_0,q_0)/\hbar}|p_2,q_2\rangle\langle p_1',q_1'|p_1,q_1\rangle \times$$
$$\langle p_0,q_0| \, e^{-c_1(q_1'-q_1)^2/2\hbar} \, e^{-c_2(p_1'-p_1)^2/2\hbar}\left\{\frac{1}{2}\left(\tilde{c}_1\tilde{c}_2 + \frac{1}{4}\right)(Q'Q + P'P) + \frac{\tilde{c}_1}{2\pi\gamma}P'Q + \tilde{c}_2\frac{\hbar\gamma}{2}Q'P\right\}^{1/2} \qquad (6.5)$$

where

$$Q' = M_{qq}' + \frac{i}{\hbar\gamma}M_{pq}', \quad Q = M_{qq} + \frac{\hbar\gamma}{i}M_{qp}$$

$$P' = M_{pp}' + \frac{\hbar\gamma}{i}M_{qp}', \quad P = M_{pp} + \frac{i}{\hbar\gamma}M_{pq} \qquad (6.6)$$

with

$$M_{qq} = \partial q_{t_1}(p_0,q_0)/\partial q_0$$
$$M_{qq}' = \partial q_{t_2}(p_1',q_1')/\partial q_1' \qquad (6.7)$$

etc., and

$$\tilde{c}_1 = c_1 + \frac{\hbar\gamma}{2}$$

$$\tilde{c}_2 = c_2 + \frac{1}{2\hbar\gamma} \qquad (6.8)$$

c_1 and c_2 are the two "Filinov parameters" that "tune" between the single and double IVR, i.e., eq 6.2 and (6.4): for $c_1 = c_2 = 0$, it is easy to see that eq 6.5 reverts to the double IVR, eq 6.2, while in the limit $c_1, c_2 \rightarrow \infty$, one has

$$e^{-c_1(q_1'-q_1)^2/2\hbar} \longrightarrow \sqrt{\frac{2\pi\hbar}{c_1}}\,\delta(q_1' - q_1)$$

$$e^{-c_2(p_1'-p_1)^2/2\hbar} \longrightarrow \sqrt{\frac{2\pi\hbar}{c_1}}\,\delta(p_1' - p_1) \qquad (6.9)$$

and it is not hard to show that eq 6.5 then collapses to the single IVR, eq 6.4; i.e., in this latter limit, $q_1' = q_1$ and $p_1' = p_1$ so that the trajectory is continuous at the intermediate time t_1, while for finite value of c_1 and c_2, there is a coordinate and momentum jump at time t_1; the size of the Filinov parameters c_1 and c_2 limits the amount of the "jump". The implementation of eq 6.5 is obvious: one chooses initial values (p_0,q_0) and evolves the trajectory to time t_1, arriving at phase point (p_1,q_1); here one jumps to a new phase point (p_1',q_1')—the distance from (p_1,q_1) being determined by Monte Carlo sampling with the Gaussian factors that limit the jump—and then evolves the trajectory to the final time t_2.

Figure 9 also shows results of this unified single-double IVR approach,[10aa] i.e., eq 6.5 (suitably modified for having operator $\hat{B} = \hat{x}$ between the two propagators, and with $t_1 = -t_2 = t$), for several values of the Filinov parameters $c \equiv c_1 = c_2$. $c = 0$ corresponds to the full double IVR (which agrees well with the full quantum result), and one sees that increasing the value of c "tunes" the result progressively toward the single (i.e., forward−backward) IVR. The calculation is more efficient the larger the value of c—because the integration over (p_1',q_1') is progressively restricted—but smaller values of c give better agreement with the correct (QM) results. One therefore has the possibility of going beyond the FB-IVR if necessary, and by a continuous degree.

Of even more relevance is that, for a system with many degrees of freedom, the Filinov parameters can be different for different degrees of freedom. Thus, one can choose large values for the "bath" degrees of freedom which are not so important, going all the way to the single (FB) IVR limit for them, while retaining the more accurate double IVR for the reaction coordinate and other important degrees of freedom. Preliminary applications suggest this to be a very fruitful way to proceed.

VII. Concluding Remarks

The initial value representation thus provides the framework for using classical molecular dynamics to implement semiclassical theory for describing quantum effects in the dynamics of complex molecular systems. The FB version of the theory, as described in section V.B. for evaluating time correlation functions, is especially attractive. The examples discussed in section V.C. show that it is capable providing an excellent

description of quantum interference effects (which are the origin, ultimately, of all quantum effects) and also the quenching of these effects (decoherence) when there is sufficiently strong coupling to environmental degrees of freedom. In proceeding with applications to real molecular systems (or at least more realistic models of them), one thus has some confidence that the FB-IVR can allow one to find out when quantum effects are important and when they are not.

An FB-IVR calculation for a typical time correlation function requires an average over the initial conditions of classical trajectories, just as a completely classical one does, plus only a one (or low) dimensional integral (over the "jump parameter"). There are some additional features, though, that increase the difficulty of an FB-IVR calculation compared to ordinary classical MD. First, the integrand for the average over initial conditions is oscillatory (though much less so than without the FB simplification). The most effective way at present for dealing with this are the various stationary phase Monte Carlo or Filinov filtering schemes (cf. eq 4.6); it would be useful to have even more efficient ways to handle this aspect of the calculation. Second, an SC-IVR calculation requires calculation of the monodromy matrixes (the matrix of derivatives of the final coordinates and momenta with respect to their initial values) in order to construct the pre-exponential factor of the IVR integrand. There have recently been several useful advances on this topic: the log-derivative algorithm,[46] which has long been recognized as the most effective way of integrating the coupled-channel Schrodinger equation for inelastic scattering, has been very fruitfully applied to calculating the pre-factor,[10bb] and Batista et al.[10r] have shown that an adiabatic approximation for computing the monodromy matrices is often quite adequate, and this greatly simplifies their calculation.

Intense effort is thus still being invested in trying to improve SC-IVR methodology, to minimize the effort required for such calculations beyond that of a completely classical treatment. There is certainly room for further development, but already the FB-IVR version of the theory is very far along this road. It should be possible to apply this approach as it presently stands to a wide variety of molecular processes, with confidence that it can reliably describe the quantum aspects of the dynamics.

References and Notes

(1) It is possible nowadays to treat equilibrium phenomena fully quantum mechanically, however, by Monte Carlo evolution of the Feyman path integral representation for the Boltzmann operator, $\exp(-\beta\hat{H})$.

(2) See, for example: (a) Billing, G. D. *J. Chem. Phys.* **1976**, *65*, 1. (b) Mavri, J.; Berendsen, H. J. C.; van Gunsteren, W. F. *J. Phys. Chem.* **1993**, *97*, 13469. (c) Hammes-Schiffer, S.; Tully, J. C. *J. Chem. Phys.* **1994**, *101*, 4657. (d) Hintenender, M.; Rebentrost, F.; Kosloff, R.; Gerber, R. B. *J. Chem. Phys.* **1996**, *105*, 11347. (e) Zdanska, P.; Schmidt, B.; Jungwirth, P. *J. Chem. Phys.* **1999**, *110*, 6246.

(3) (a) Feynman, R. P.; Hibbs, A. R. *Quantum Mechanics and Path Integrals*; Mc-Graw Hill: New York, 1965; pp 279−286. (b) Doll, J. D.; Myers, L. E. *J. Chem. Phys.* **1979**, *71*, 2880. (c) Feynman, R. P.; Kleinert, H. *Phys. Rev. A* **1986**, *34*, 5080; Janke, W.; Kleinert, H. *Chem. Phys. Lett.* **1987**, *137*, 162. (d) Jang, S.; Voth, G. A. *J. Chem. Phys.* **1999**, *111*, 2357, 2371, and many references therein.

(4) (a) Miller, W. H. *J. Chem. Phys.* **1970**, *53*, 1949. (b) Miller, W. H. *J. Chem. Phys.* **1970**, *53*, 3578. (c) Miller, W. H. *Chem. Phys. Lett.* **1970**, *7*, 431. (d) Miller, W. H. *Adv. Chem. Phys.* **1974**, *25*, 69; **1975**, *30*, 77.

(5) (a) Marcus, R. A. *Chem. Phys. Lett.* **1970**, *7*, 252. (b) Marcus, R. A. *J. Chem. Phys.* **1971**, *54*, 3965. (c) Marcus, R. A. *J. Chem. Phys.* **1972**, *56*, 3548. (d) Kreek, H.; Marcus, R. A. *J. Chem. Phys.* **1974**, *61*, 3308. (e) Fitz, D. E.; Marcus, R. A. *J. Chem. Phys.* **1973**, *59*, 4380.

(6) (a) Herman, M. F.; Kluk, E. *Chem. Phys.* **1984**, *91*, 27−34. (b) Herman, M. F. *Chem. Phys. Lett.* **1997**, *275*, 445−452.

(7) (a) Campolieti, G.; Brumer, P. *Phys. Rev. A* **1994**, *50*, 997−1018. (b) Campolieti, G.; Brumer, P. *J. Chem. Phys.* **1998**, *109*, 2999−3003. (c) Campolieti, G.; Brumer, P. *J. Chem. Phys.* **1997**, *107*, 791−803. (d) McQuarrie, B. R.; Brumer, P. *Chem. Phys. Lett.* **2000**, *319*, 27−44. (e) Batista, V. S.; Brumer, P. *J. Phys. Chem.*, in press.

(8) (a) Kay, K. G.; *J. Chem. Phys.* **1994**, *100*, 4377−4392. (b) Kay, K. G. *J. Chem. Phys* **1994**, *100*, 4432−4445. (c) Kay, K. G. *J. Chem. Phys.* **1997**, *107*, 2313−2328. (d) Elran, Y.; Kay, K. G. *J. Chem. Phys.* **1999**, *110*, 8912−8918. (e) Elran, Y.; Kay, K. G. *J. Chem. Phys.* **1999**, *110*, 3653−3659. (f) Kay, K. G. *J. Chem. Phys.* **1994**, *101*, 2250−2260.

(9) (a) Heller, E. J. *J. Chem. Phys.* **1991**, *94*, 2723−2729. (b) Sepulveda, M. A.; Tomsovic, S.; Heller, E. J. *Phys. Rev. Lett.* **1992**, *69*, 402−405. (c) Tomsovic, S.; Heller, E. J. *Phys. Rev. Lett.* **1991**, *67*, 664−667.

(10) (a) Miller, W. H. *J. Chem. Phys.* **1991**, *95*, 9428−9430. (b) Keshavamurthy, S.; Miller, W. H. *Chem. Phys. Lett.* **1994**, *218*, 189−194. (c) Spath, B. W.; Miller, W. H. *J. Chem. Phys.* **1996**, *104*, 95−99. (d) Spath, B. W.; Miller, W. H. *Chem. Phys. Lett.* **1996**, *262*, 486-494. (e) Sun, X.; Miller, W. H. *J. Chem. Phys.* **1997**, *106*, 916−927. (f) Sun, X.; Miller, W. H. *J. Chem. Phys.* **1997**, *106*, 6346−6353. (g) Batista, V. S.; Miller, W. H. *J. Chem. Phys.* **1998**, *108*, 498−510. (h) Miller, W. H. The Semiclassical Initial Value Representation for Including Quantum Effects in Molecular Dynamics Simulations. In *Classical and Quantum Dynamics in Condensed Phase Simulations*; B. J. Berne, G. Ciccotti, D. F. Coker, Eds.; World Scientific: Singapore, 1998; pp 617−627. (i) Sun, X.; Miller, W. H. *J. Chem. Phys.* **1998**, *108*, 8870−8877. (j) Wang, H.; Sun, X.; Miller, W. H. *J. Chem. Phys.* **1998**, *108*, 9726−9736. (k) Sun, X.; Wang, H.; Miller, W. H. *J. Chem. Phys.* **1998**, *109*, 4190−4200. (l) Sun, X.; Wang, H.; Miller, W. H. *J. Chem. Phys.* **1998**, *109*, 7064−7074. (m) Miller, W. H. *J. Chem. Soc., Faraday Discuss.* **1998**, *110*, 1−21. (n) Wang, H.; Song, X.; Chandler, D.; Miller, W. H. *J. Chem. Phys.* **1999**, *110*, 4828−4840. (o) Skinner, D.; Miller, W. H. *Chem. Phys. Lett.* **1999**, *300*, 20−26. (p) Batista, V. S.; Zanni, M. T.; Greenblatt, B. J.; Neumark, D. M.; Miller, W. H. *J. Chem. Phys.* **1999**, *110*, 3736−3747. (q) Sun, X.; Miller, W. H. *J. Chem. Phys.* **1999**, *110*, 6635−6644. (r) Guallar, V.; Batista, V. S.; Miller, W. H. *J. Chem. Phys.* **1999**, *110*, 9922−9936. (s) Miller, W. H. *J. Phys. Chem.* **1999**, *103*, 9384−9387. (t) Skinner, D. E.; Miller, W. H. *J. Chem. Phys.* **1999**, *111*, 10787−10793.(u) Wang, H.; Thoss, M.; Miller, W. H. *J. Chem. Phys.* **2000**, *112*, 47−55. (v) Coronado, E. A.; Batista, V. S.; Miller, W. H. *J. Chem. Phys.* **2000**, *112*, 5566−5575. (w) Thoss, M.; Miller, W. H.; Stock, G. *J. Chem. Phys.* **2000**, *112*, 10282−10292. (x) Guallar, V.; Batista, V. S.; Miller, W. H. *J. Chem. Phys.* **2000**, *113*, 9510−9522.. (y) Gelabert, R.; Gimenez, X.; Thoss, M.; Wang, H. B.; Miller, W. H. *J. Chem. Phys.* **2001**, *114*, 2572−2579. (z) Wang, H.; Thoss, M.; Sorge, K.; Gelabert, R.; Gimenez, X.; Miller, W. H. *J. Chem. Phys.* **2001**, *114*, 2562−2571. (aa) Thoss, M.; Miller, W. H. *J. Chem. Phys.*, in press. (bb) Gelabert, R.; Gimenez, X.; Thoss, M.; Wang, H.; Miller, W. H. *J. Phys. Chem. A* **2000**, *104*, 10321.

(11) (a) Walton, A. R.; Manolopoulos, D. E. *Mol. Phys.* **1996**, *87*, 961−978. (b) Walton, A. R.; Manolopoulos, D. E. *Chem. Phys. Lett.* **1995**, *244*, 448−455. (c) Brewer, M. L.; Hulme, J. S.; Manolopoulos, D. E. *J. Chem. Phys.* **1997**, *106*, 4832−4839.

(12) (a) Garashchuk, S.; Tannor, D. *Chem. Phys. Lett.* **1996**, *262,* 477−485. (b) Garashchuk, S.; Grossmann, F.; Tannor, D. J. *J. Chem. Soc., Faraday Trans.* **1997**, *93*, 781−789 1997. (c) Garashchuk, S.; Tannor, D. J. *PCCP* **1999**, *1*, 1081−1090. (d) Garashchuk, S.; Tannor, D. J. *Annu. Rev. Phys. Chem.* **2000**, *51*, 553−600.

(13) (a) Grossman, F. *Phys. Rev. A* **1998**, *57*, 3256−3261. (b) Grossman, F. *Chem. Phys. Lett.* **1996**, *262*, 470−476. (c) Sepulveda, M. A.; Heller, E. J. *J. Chem. Phys.* **1994**, *101*, 8004−8015.

(14) (a) Shalashilin, D. V.; Jackson, B. *Chem. Phys. Lett.* **1998**, *291*, 143−152. (b) Shalashilin, D. V.; Jackson, B. *Chem. Phys. Lett.* **2000**, *318*, 305−313.

(15) (a) Cao, J.; Voth, G. A. *J. Chem. Phys.* **1996**, *104*, 273. (b) Hernandez, R.; Voth, G. A. *Chem. Phys.* **1998**, *233*, 243. (c) Ovchinnikov, M.V.; Apkarian, A.; Voth, G. A. *J. Chem. Phys.*, in press.

(16) Berne, B. J.; Harp, G. D. *Adv. Chem. Phys.* **1970**, *17*, 63−227.

(17) Also see the discussion in refs 9a and 10a.

(18) (a) Van Vleck, J. V. *Proc. Nat. Acad. Sci. U.S.A.* **1928**, *14*, 178. (b) Gutzwiller, M. C. *Chaos in Classical and Quantum Mechanics*; Springer: New York, 1990.

(19) It was discussed many years ago [Miller, W. H.; George, T. F. *J. Chem. Phys.* **1972**, *56*, 5668 (cf. Appendix D)] that although the SC approximation has the same formal structure in any representation (cf. ref 4d), it may in fact be more accurate in some representations than in others;

Feature Article

J. Phys. Chem. A, Vol. 105, No. 13, 2001 **2955**

e.g., for the harmonic oscillator, the SC approximation for the time propagator is exact in Cartesian coordinate (or momentum) space, while it is not so in action−angle variable space. Similarly, the SC approximation for the fixed energy propagator, i.e., the Green's function, $\langle \mathbf{x}_2 | \hat{G}(E) | \mathbf{x}1 \rangle = (i\hbar)^{-1} \int_0^\infty dt \, e^{iEt/\hbar} \langle \mathbf{x}_2 | e^{-i\hat{H}t/\hbar} | \mathbf{x}_1 \rangle$, which is obtained by the performing the time integral by the SPA, is not exact (even for the harmonic oscillator). The IVR model thus effectively assumes that the SC approximation is best in Cartesian coordinate/momentum space and the time representation.

(20) (a) Davis, M. J.; Heller, E. J. *J. Chem. Phys.* **1981**, *75*, 246. (b) Heller, E. J. *J. Chem. Phys.* **1975**, *62*, 1544. (c) Heller, E. J. *Acc. Chem. Res.* **1981**, *14*, 368.

(21) (a) Glauber, R. J. *Phys. Rev.* **1963**, *130*, 2529; *131*, 2766. (b) Klauder, J. R.; Skagerstam, B. S. *Coherent States*; World Scientific: River Edge, NJ, 1985.

(22) Meyer, H. D.; Miller, W. H. *J. Chem. Phys.* **1979**, *70*, 3214.

(23) There is also a version of this for the adiabatic representation, for which we refer the reader to ref 22.

(24) See, for example: Raff, L. M.; Thompson, D. L. In *The Theory of Reaction Dynamics*; M. Baer, Ed.; CRC Press: Boca Raton, FL, 1985; Vol. 3, p 1.

(25) Meyer, H. D.; Miller, W. H. *J. Chem. Phys.* **1979**, *71*, 2156.

(26) Orel, A. E.; Ali, D. P.; Miller, W. H. *Chem. Phys. Lett.* **1981**, *79*, 137.

(27) Gray, S. K.; Miller, W. H. *Chem. Phys. Lett.* **1981**, *79*, 137.

(28) See, for example: Hack, M. D.; Truhlar, D. G. *J. Chem. Phys.* **2000**, *104*, 7917.

(29) M & M also discussed a semiclassical version of the model in ref 22, though not the IVR version of SC theory. They showed that for two-state curve-crossing problems, the SC version of their model was a considerable improvement over the quasiclassical version.

(30) In the original applications of this model in ref 22, classical trajectories (in the full space of nuclear and electronic degrees of freedom) were actually integrated in these Cartesian variables; i.e., initial quasiclassical conditions were specified in the electronic action−angle variables, transformed to the Cartesian initial conditions and integrated, and then transformed back to action−angle variables at the end of the trajectory.

(31) (a) Stock, G.; Thoss, M. *Phys. Rev. Lett.* **1997**, *78*, 578. (b) Thoss, M.; Stock, G. *Phys. Rev. A* **1999**, *59*, 64.

(32) Pechukas, P. *Phys Rev.* **1969**, *181*, 174.

(33) Beck, C.; Schinke, R.; Woywod, C.; Domcke, W. *J. Chem. Phys.* **1997**, *107*, 7296.

(34) Secrest, D.; Johnson, B. R. *J. Chem. Phys.* **1966**, *45*, 4556.

(35) See, for example: Rankin, C. C.; Miller, W. H. *J. Chem. Phys.* **1971**, *55*, 3150.

(36) Stine, J. R.; Marcus, R. A. *Chem. Phys. Lett.* **1974**, *29*, 575.

(37) (a) Filinov, V. I. *Nucl. Phys.* **1986**, *B271*, 717−725. (b) Makri, N.; Miller, W. H. *Chem. Phys. Lett.* **1987**, *139*, 10−14. (c) Doll, J. D.; Freeman, D. L. *Adv. Chem. Phys.* **1989**, *73*, 289−304.

(38) (a) Miller, W. H. *J. Chem. Phys.* **1975**, *62*, 1899. (b) Miller, W. H.; Schwartz, S. D.; Tromp, J. W. *J. Chem. Phys.* **1983**, *79*, 4889.

(39) Wigner, E. *Phys. Rev.* **1932**, *40*, 749−759.

(40) (a) Miller, W. H. *J. Chem. Phys.* **1974**, *61*, 1823. (b) Heller, E. J. *J. Chem. Phys.* **1976**, *65*, 1289. (c) Brown, R. C.; Heller, E. J. *J. Chem. Phys.* **1981**, *75*, 186. (d) Lee, H. W.; Scully, M. O. *J. Chem. Phys.* **1980**, *73*, 2238. (e) Cline, R. E., Jr.; Wolynes, P. G. *J. Chem. Phys.* **1988**, *88*, 4334. (f) Khidekel, V.; Chernyak, V.; Mukamel, S. In *Femtochemistry: Ultrafast Chemical and Physical Processes in Molecular Systems*; Majed Chergui, Ed.; World Scientific: Singapore, 1996; p 507.

(41) (a) Pollak, E.; Liao, J. L. *J. Chem. Phys.* **1998**, *108*, 2733−2743. (b) Pollak, J. L.; Liao, J. L. *J. Chem. Phys.* **1999**, *110*, 80−87.

(42) (a) Makri, N.; Thompson, K. *Chem. Phys. Lett.* **1998**, *291*, 101−109. (b) Makri, N.; Thompson, K. *J. Chem. Phys.* **1999**, *110*, 1343−1353. (c) Makri, N.; Thompson, K. *Phys. Rev. E* **1999**, *59*, R4729−R4732. (d) Shao, J.; Makri, N. *J. Phys. Chem. A* **1999**, *103*, 7753−7756. (e) Shao, J.; Makri, N. *J. Phys. Chem. A* **1999**, *103*, 9479−9486. (f) Shao, J.; Makri, N. *J. Chem. Phys.* **2000**, *113*, 3681.

(43) Husimi, K. *Proc. Phys. Math. Soc. Jpn.* **1940**, *22*, 264−314.

(44) For quenching of glory oscillations, see: (a) Olson, R. E.; Bernstein, R. B. *J. Chem. Phys.* **1958**, *49*, 162. (b) Cross, R. J., Jr. *J. Chem. Phys.* **1968**, *49*, 1976. (c) Miller, W. H. *J. Chem. Phys.* **1969**, *50*, 3124.

(45) For a more general discussion of quenching of interference, see: Miller, W. H. *J. Chem. Phys.* **1971**, *54*, 5386.

(46) (a) Johnson, B. R. *J. Comput. Phys.* **1973**, *13*, 445. (b) Manolopoulos, D. E. *J. Chem. Phys.* **1986**, *85*, 6425.